NATIONAL ADVISORY COMMITTEE FOR AERONAUTICS

TECHNICAL NOTE

No. 944

EFFECT OF CURVATURE ON STRENGTH OF AXIALLY LOADED

SHEET-STRINGER PANELS

By Walter Ramberg, Samuel Levy, and Kenneth L. Fienup
National Bureau of Standards

Washington
August 1944

NATIONAL ADVISORY COMMITTEE FOR AERONAUTICS

TECHNICAL NOTE NO. 944

EFFECT OF CURVATURE ON STRENGTH OF AXIALLY LOADED

SHEET-STRINGER PANELS

By Walter Ramberg, Samuel Levy, and Kenneth L. Fienup

SUMMARY

Compressive tests were made on twenty-one 24S-T aluminum-alloy sheet-stringer panels 12 inches in length and 16 inches in developed width, reinforced by four Z stringers spaced 4 inches apart. The radii of curvature R ranged from 19 inches to infinity, the sheet thicknesses t from 0.025 to 0.190 inch, and the rivet spacing from 0.5 to 2 inches.

The curvature increased the strain for buckling of sheet between stringers up to 5.35 times. The critical strain for the panels with the heavy sheet covering a range of values of b^2/Rt (b = stringer spacing) up to 6.4 agreed with the range of values computed from NACA Technical Note No. 895 for curved sheet with simply supported edges and with a formula given by Leggett for simple support. The critical strain for the panels with the thin sheet covering a range of values of b^2/Rt up to 32.5 agreed with another formula by Leggett for clamped support. Panels of intermediate thickness covering a range of values of b^2/Rt up to 16 buckled at strains given approximately by Wenzek's formula.

The critical strain for buckling between rivets in the elastic range increased 100 percent with an increase of b^2/Rt from 0 to 32.6.

The curvature of the panels generally increased the effective width after buckling, particularly at strains close to the buckling strain. At much larger strains the effective width for the curved sheet approached Marguerre's formula for flat sheet with simply supported edges.

Fifteen of the panels failed by stringer instability, two failed by separation of rivets, three failed by buckling of stringers and sheet as a unit, and one failed by buckling of sheet between stringers.

The strength of the panels did not differ by more than 6 percent from that computed from the nomogram in NACA Technical Note No. 856 for flat panels of the same design except for two panels which failed at loads 9 and 15 percent greater than the computed loads.

INTRODUCTION

An understanding of the possible beneficial effect of curvature on the strength of axially loaded sheet-stringer panels is important in the construction of airplane wings and fuselages from reinforced curved sheet.

The large-deflection theory of curved sheet is presented in reference 1 for the special case of simple support along the edges of the sheet. It was concluded from this theory that initial curvature may cause an appreciable increase in the buckling load but that initial curvature causes a negligibly small change in the effective width for edge strains which are several times the buckling strain.

The results of the theory are compared in reference 1 with experimental results by Cox and Clenshaw, Newel, Ebner, and Wenzek. The comparison indicates a qualitative agreement with the theory. However, the edge conditions for the various tests varied so widely as to make impossible a direct quantitative check of the analysis.

The experimental results obtained are not directly comparable with the results obtained by previous investigators on the strength of curved sheet. Most previous experimenters tested specimens with but a single bay, in which a large amount of lateral motion of the edges was possible. In this work the specimens had several bays and so the lateral motion of the edges was probably much less.

The tests described in this paper were made at the request and with the financial assistance of the National Advisory Committee for Aeronautics. The object of this study was to provide experimental data under carefully controlled conditions which could be used to check the adequacy

of the theory, and beyond that to furnish data for empirical charts of the buckling load, effective width, and ultimate load of curved sheet-stringer panels.

SYMBOLS

The symbols have the following significance:

R radius of curvature of sheet

b stringer spacing

t sheet thickness

l length of panel

L rivet spacing

ϵ strain at stringer centroid

ϵ' strain at point of contact of sheet and stringers

ϵ_{cr} strain for buckling of sheet between stringers

σ_{cr} critical stress

E Young's modulus

μ Poisson's ratio

P_{sh} sheet load between adjacent stringers

σ_s stress in sheet at stringer line

w/b effective width ratio

APPARATUS AND TESTS

Panels.- The dimensions of the panels are given in table 1 and in figure 1. The stringers, the sheet, and the rivets were 24S-T aluminum alloy. The stringers were nominally of the same dimensions for all the panels. Actually their cross-sectional area varied between 0.163 and 0.193 square inch. The thickness of the sheet in the panels was

taken as the average of ten readings. The variation of
sheet thickness in a given panel did not exceed 0.001 inch.
The area of the panels was determined from the weight, den-
sity, and length after correcting the weight for the weight
of the rivet heads. This area checked the area obtained
from cross-sectional dimensions within 1/2 percent.

Panels 4, 5, and 6 with rivet spacings nominally 20,
40, and 80 times the sheet thickness were included to deter-
mine the effect of rivet pitch on the strength of curved
panels. Panels 17 to 21 with a sheet thickness of 3/16 inch
were included to determine the effect of relatively large
sheet thickness.

Mechanical properties of material.- Tensile tests and
single-thickness compressive tests (reference 2) were made
on specimens from the sheet used in the panels. For some of
the material pack compressive tests (reference 3) were also
made. The resulting stress-strain curves are given in fig-
ure 2, and the mechanical properties are given in table 2.
The single-thickness compressive tests and the pack compres-
sive tests gave identical results within the observational
error.

Compressive properties of the stringers were determined
from compressive tests of 21 unidentified 4-inch lengths of
the stringer stock. The resulting family of compressive
stress-strain curves is plotted at A in figure 3. Of this
family, more than half agree with the single stress-strain
curve B. This curve was used for computations for all the
panels since the correspondence between the stringer samples
and the panels was unfortunately not available. Except for
2 of the 21 curves, the deviation from curve B was less than
1 percent. For the remaining 2 curves the differences in
modulus were 2 and 3 percent and the differences in yield
strength (0.002 offset) were 5 and 6 percent.

Preparation of panels.- The panels, as received, were
rolled to approximately the correct radius of curvature.
They were prepared for test by clamping them in a supporting
jig having the correct radius of curvature. The jig was
then mounted in a grinder and the ends of the panel were
ground flat and parallel. After grinding, the panel was
clamped between ground steel blocks with the supporting jig
still attached. In some of the panel tests Wood's metal was
cast around the ends of the panel to prevent local crinkling;
in the other panel tests this step was omitted. No difference
in behavior at the ends in the two instances was observed.

In some of the panel tests wire-type strain gages were used. These strain gages were attached to the stringers with Duco cement and the cement was allowed to dry 1 to 2 days.

Mounting panels in testing machine.- Some of the tests were made in a 120,000-pound vertical testing machine and the remainder in a 200,000-pound vertical testing machine. The panel was placed with its centroidal axis along the center line of the machine. A plaster cap was then cast between the top ground-steel block and the upper head of the testing machine at a load of about 300 pounds.

After the plaster cap had set, the supporting jig was removed and edge guides were attached. The edge guides approximated the support of the sheet at the stringers; they allowed the edge of the sheet to move freely in its own plane but prevented lateral displacements. Details of construction of these guides are shown in figure 8 of reference 4.

Strain measurements.- Eight 2-inch Tuckerman strain gages were attached to the stringers of the panel. Four of these gages were attached directly to the outstanding flanges. The remaining four gages measured the strain on the stringer flange joined to the sheet using the lever strain transfers described on page 4 of reference 5.

In the tests it was found that the buckling was sometimes so violent that the Tuckerman gages were thrown out of adjustment so that the increment in strain during the process of buckling could not be measured by these gages. In order to measure the increment in strain during buckling, SR-4 electric strain gages were also attached to the stringers for some of the panel tests.

Figure 4 shows one of the panels set up for test with the strain gages attached. The SR-4 wire strain gages are on the under side of the stringers and therefore are not visible in the photograph.

Figure 5 shows the location of the strain gages on the stringer cross section. The strain ϵ at the centroid of the stringer and the strain ϵ' at the point of contact of the sheet and the stringer were computed from the measured strains on the assumption that the strain in the stringer varied linearly with the distance from the sheet. This assumption of linear strain variation was partially checked by

attaching twelve SR-4 gages to a single stringer and testing it under axial loads. No deviation from linear strain variation across the section was observed until after severe bending at an axial stress of 40,000 pounds per square inch.

Buckling.- The buckling of the sheet between stringers, the buckling of the sheet between rivets, and the twisting of the stringers was noted by frequent visual inspection.

Test schedule.- After mounting the panel in the testing machine, the strain was measured for small increments in load. At a load of about 10 percent of the expected maximum load, those panels which did not show a uniform strain distribution were removed from the testing machine and their ends were reground. They were then tested again. For the remaining panels the loading was continued up to failure, and strains were read for small increments in the load.

RESULTS OF TESTS

Strains.- The load-strain graphs are shown in figures 6 to 26. The stringer strains are the strains ϵ at the centroids of the stringers and the sheet strains are the strains ϵ' in the extreme fiber of the stringer at the contact between stringer and sheet. Notes on the progress of buckling appear on the figures.

The strains read on the SR-4 wire-type strain gages differed from the strains read on the Tuckerman strain gages by amounts up to 2 percent; the differences were small enough to be explained by local variations of the strain in stringers and sheet. Increments in strain were taken from the Tuckerman gage readings except in those cases where the Tuckerman gages were thrown out of adjustment by buckling or by accidental jarring; in such cases the strain increments were taken from readings of the SR-4 strain gages.

Permanent set readings were taken for some of the panel tests. The readings are shown on the load-strain graphs.

Buckling.- The strains at which buckling was first noticed are given in table 3. For nearly 80 percent of the panels, the buckling was of the "snap diaphragm" type. Two kinds of buckling of the sheet between stringers were observed. For the slightly curved panels, the buckles extended

from stringer to stringer just as for flat panels, while, for the more curved panels, some of the buckles extended only part of the way from stringer to stringer as in a thin-walled cylinder under axial load.

In addition to buckling of the sheet between stringers, there was buckling of the sheet between rivets, instability of the stringers, and buckling of the panel as a whole between edge guides. The last type of buckling occurred only in panels with 0.188-inch sheet. In these panels the sheet was so thick relative to the stringers that the stringers were unable to restrain the sheet against normal displacement at the rivet line.

The buckle pattern in the sheet did not stay fixed as the load increased. Buckling between stringers became more general and the buckle separation decreased as the load increased. In some cases, changes in the buckle pattern were observed at loads as high as four to five times the first buckling load. In panel 1, for example, buckling started at 5 kips and changes in the buckle pattern occurred at 6.9, 8.2, 8.9, 10.6, and 22.1 kips. Figures 27 and 28 show the buckle pattern in panel 1 at a load of 30.0 kips.

Failure.- The maximum load, the average stress at failure, the average stringer stress at failure, the average sheet strain at failure, and the type of failure are summarized in table 4.

ANALYSIS

Buckling of sheet between stringers.- A theoretical value for the strain for buckling between stringers ϵ_{cr} was obtained upon the assumption that the sheet was elastic and would buckle like an infinitely long curved plate of constant width and constant thickness, simply supported at the edges. In figures 8, 9, and 10 of reference 1 curves are given for the effective width of such a plate. These curves are redrawn in figure 29. The curves indicate that buckling can occur as follows for simply supported sheet:

$$\left.\begin{array}{l} b^2/Rt = 0; \quad \epsilon_{cr}b^2/t^2 = 3.66 \\[2mm] b^2/Rt = 5; \quad 4.9 \leqq \epsilon_{cr}b^2/t^2 \leqq 5.1 \\[2mm] b^2/Rt = 10; \quad 6.2 \leqq \epsilon_{cr}b^2/t^2 \leqq 8.1 \end{array}\right\} \tag{1}$$

where

b   stringer spacing

R   radius of curvature

t   sheet thickness

ϵ_{cr} critical buckling strain

The limiting values of critical strain when $b^2/Rt = 5$ and 10 indicate a range within which the sheet can be in stable equilibrium in either the buckled or unbuckled state. Above this range the sheet must be buckled and below it the sheet must be unbuckled.

An approximate value of the critical buckling strain for a long curved plate of constant width and thickness having clamped edges was computed on the assumption that the buckling strain would be increased in the ratio of the critical strains of clamped and simply supported flat sheet. On this basis the critical strain for clamped curved sheet is given by:

$$\left. \begin{array}{l} b^2/Rt = 0; \quad \epsilon_{cr}b^2/t^2 = 6.37 \\[2mm] b^2/Rt = 5; \quad 8.5 \leqq \epsilon_{cr}b^2/t^2 \leqq 8.9 \\[2mm] b^2/Rt = 10; \ 10.8 \leqq \epsilon_{cr}b^2/t^2 \leqq 14.1 \end{array} \right\} \tag{2}$$

The values of critical strain given by equations (1) and (2) are plotted in figure 30 for the preceding values of b^2/Rt together with the measured values. Open points denote panels which buckled inside of the elastic range ($\epsilon_{cr} < 0.0032$) and solid points denote panels which buckled beyond that range ($\epsilon_{cr} > 0.0032$). Panels 17 to 19 were omitted since they did not buckle between stringers.

Wenzek's equation for critical stress (reference 6)

$$\sigma_{cr} = 5 \, E(t/b)^2 + 0.3 \, E(t/R) \tag{3}$$

is based on tests that permitted lateral motion of the edges of the sheet. In the elastic range it can be rewritten as:

$$\epsilon_{cr}b^2/t^2 = 5.0 + 0.3 \, b^2/Rt \tag{4}$$

This equation is plotted as curve A in figure 30 for comparison with the observed data.

Leggett's curves for critical stress (reference 7, figure 1) are plotted as curves B and C in figure 30 for simple and clamped edge support, respectively. Leggett obtained his results assuming no lateral motion of the edges of the sheet by solving the equilibrium equations and showed that they agree closely with those of Redshaw (reference 8) who uses energy methods. Leggett points out (reference 7, p. 5) that his results are only applicable when "b/R is small." In the present tests the value of b/R varied from 0 for panels 9, 14, and 21 to 0.209 for panels 6, 7, 8, 13, 20, and 27.

Stowell's equation (reference 9, equation (13)) for critical stress is intended for use where lateral motion of the edges of the sheet is permitted. For the case when b^2/Rt is large it is:

$$\sigma_{cr} = \frac{k_\infty \pi^2 E t^2}{12(1-\mu^2)b^2} \; \frac{1 + \sqrt{1 + \frac{48(1-\mu^2)}{\pi^4}\left(\frac{b^2}{Rtk_\infty}\right)^2}}{2} \tag{5}$$

where k_∞ is determined from the condition that

$$\sigma_{cr_\infty} = \frac{k_\infty \pi^2 E t^2}{12(1-\mu^2)b^2}$$

when $R = \infty$. Taking $\mu^2 = 0.1$, equation (5) can be rewritten in the elastic range for the case of simply supported edges where $k_\infty = 4.00$ as

$$\epsilon_{cr}b^2/t^2 = 1.83\left(1 + \sqrt{1 + 0.0277(b^2/Rt)^2}\right) \tag{6}$$

and for the case of clamped edge support where $k_\infty = 6.97$ as

$$\epsilon_{cr}b^2/t^2 = 3.185\left(1 + \sqrt{1 + 0.00912(b^2/Rt)^2}\right) \tag{7}$$

Equations (6) and (7) are plotted as curves D and E, respectively, in figure 30. Stowell, in addition, gives an equation (reference 9, equation (10))

$$\sigma_{cr} = \frac{k_\infty \pi^2 E t^2}{12(1 - \mu^2)b^2} + \frac{E b^2}{k_\infty \pi^2 R^2} \tag{8}$$

which he recommends for use when b^2/Rt is small. Taking $\mu^2 = 0.1$, this equation can be rewritten in the elastic range for the case of simply supported edges where $k_\infty = 4.00$ as

$$\epsilon_{cr} b^2/t^2 = 3.66 + 0.0253(b^2/Rt)^2 \tag{9}$$

and for the case of clamped edge support where $k_\infty = 6.97$ as

$$\epsilon_{cr} b^2/t^2 = 6.37 + 0.0145(b^2/Rt)^2 \tag{10}$$

Equations (9) and (10) are plotted as curves F and G, respectively, in figure 30.

Lundquist and Schuette (reference 14) recommend that the critical compressive stress for a curved sheet between stiffeners where lateral motion of the edges of the sheet is permitted be taken as the larger of the following values:

(a) The critical compressive stress for an unstiffened circular cylinder of the same radius-thickness ratio

(b) The critical compressive stress for the same sheet when flat

They give on page 13 of reference 14 for condition (a) as two possible values

$$\epsilon_{cr} = \frac{\sigma_{cr}}{E} = 0.605 \frac{t}{R} \quad \text{and} \quad \epsilon_{cr} = \frac{\sigma_{cr}}{E} = 0.363 \frac{t}{R}$$

These conditions may be rewritten as

$$\epsilon_{cr} \frac{b^2}{t^2} = 0.605 \frac{b^2}{tR} \tag{11a}$$

and

$$\epsilon_{cr} \frac{b^2}{t^2} = 0.363 \frac{b^2}{tR} \tag{11b}$$

Condition (b) may be expressed as

$$\epsilon_{cr} \frac{b^2}{t^2} = 3.66 \qquad (12a)$$

for plates having simply supported edges and as

$$\epsilon_{cr} \frac{b^2}{t^2} = 6.37 \qquad (12b)$$

for plates having clamped edges. Equations (11a), (11b), (12a), and (12b) are plotted as curves H, J, K, and L, respectively, in figure 30.

Figure 30 shows a large variation in the observed buckling strain even when panels 14, 15, 16, 20, and 21 which buckled in the plastic range are excluded. The critical strain ratio varied from $\epsilon_{cr} b^2/t^2 = 4.2$ for panel 12 having $b^2/Rt = 0$ to $\epsilon_{cr} b^2/t^2 = 24.6$ for panel 4 having $b^2/Rt = 32.6$.

Comparison of the curves for simple edge support (curves B, D, F, and K together with H or J, fig. 30) with the observed data on panels 12 and 13 having relatively thick sheet (t/b = 0.025), approximating the condition of simply supported edges, indicates that over the range covered by the data $0 < b^2/Rt < 2.2$ only curve B agrees within the experimental scatter of about 10 percent. The remaining curves are lower as might be expected since they apply to cases where lateral motion of the edges of the sheet is permitted.

Comparison of the curves for clamped edge support (curves C, E, G, and L together with H or J, fig. 30) with the observed data on panels 1 to 6 having relatively thin sheet (t/b = 0.0062) approximating the condition of clamped support at the edges, indicates that over the entire range covered by the data $0 < b^2/Rt < 32.5$ Leggett's curve C gives the best fit. Again, the remaining curves are lower as might be expected since they apply to cases where lateral motion of the edges of the sheet is permitted.

Figure 30 indicates that Wenzek's formula, curve A, gives an approximate value of critical strain for $b^2/Rt < 16$. In the case of panel 4 for which the stringer supplied nearly clamped support to the sheet, Wenzek's formula is 40

percent low; while in the case of panel 13 for which the
stringer supplied nearly simple support to the sheet,
Wenzek's formula is 23 percent high.

Curvature caused the greatest increase in critical
buckling strain for panels 4, 5, and 6. These panels had a
radius of curvature of 19.1 inches. The critical strains
for buckling between stringers of panels 4, 5, and 6 were
0.00101, 0.00100, and 0.00087, respectively. Panels 7, 8,
and 9 of reference 4 were nominally the same as panels 4, 5,
and 6 of the present report except that they were flat.
Their critical buckling strains were 0.00033, 0.00025, and
0.00020, respectively. The curvature therefore caused in-
creases in critical buckling strain by a factor of 3.06,
4.00, and 4.35, respectively. Figure 30 indicates that even
greater increases in buckling strain might be expected from
further increases in curvature.

Buckling of sheet between rivets.- The experimental
values of strain for buckling of sheet between rivets are
plotted in figure 31 against the ratio L/t of rivet spac-
ing to sheet thickness. The curve in figure 31 is faired
through experimental values of buckling strain for flat
24S-T aluminum-alloy panels; it was copied from curve C,
figure 49 of reference 4. It is evident from figure 31 that
panel 6, having a value of b^2/Rt of 32.6, buckled between
rivets in the elastic range at a strain 100 percent larger
than the corresponding strain for flat panels. The remain-
ing panels had rivet spacings L/t between 15 and 40 and
all buckled at strains in the plastic range, in which a con-
siderable scatter due to eccentricities may be expected.
The scatter of points in this range in figure 31 is, in fact,
too large to reveal any consistent increase in buckling
strain with increasing curvature; however, the average buck-
ling strain was considerably larger than for the flat panels.

Effective width of curved sheet.- The effective width
w of the sheet in the three center bays of the panels was
computed from the equation

$$w = \frac{P_{sh}}{t\sigma_s} \tag{13}$$

where

P_{sh} sheet load between adjacent stringers, average for
three center bays

σ_s longitudinal compressive stress corresponding to strain ϵ' (fig. 2) on sheet side of stringer

The sheet load P_{sh} was calculated by subtracting the load carried by the stringers and the load carried by the edge bays from the applied load and dividing by 3 (corresponding to the three center bays). The load on each stringer was obtained from the average stringer strain, the compressive stress-strain curve of the stringer material (curve B, fig. 3), and the cross-sectional area of the stringer (table 1). Except for panels 4, 5, and 6, the load carried by the edge bays was obtained from Marguerre's formula, (reference 11, p. 45)

$$\left. \begin{aligned} w/b &= 1, & \epsilon' &\leq 3.64\,(t/b)^2 \\ w/b &= 1.54\,(t^2/b^2\epsilon')^{1/3}, & \epsilon' &\geq 3.64\,(t/b)^2 \end{aligned} \right\} \quad (14)$$

where b is the width of the bay. For panels 4, 5, and 6, which had a large b^2/Rt ratio even in the narrow edge bays, the load carried by the edge bays was computed either from Wenzek's formula (reference 6)

$$\left. \begin{aligned} w/b &= 1, & \epsilon' &\leq (5 + 0.3b^2/Rt)(t/b)^2 \\ w/b &= (5 + 0.3b^2/Rt)^{1/2} \Big/ (\epsilon'b^2/t^2)^{1/2} \\ &\quad -(b/R)\left[1 - (5 + 0.3b^2/Rt) \Big/ (\epsilon'b^2/t^2)\right], \\ \epsilon' &\geq (5 + 0.3b^2/Rt)(t/b)^2 \end{aligned} \right\} \quad (15)$$

or from Marguerre's formula, equation (14), for simply supported sheet, choosing whichever formula gave the larger value of effective width.

The observed effective width is plotted in figures 32 to 36 in terms of the dimensionless ratios $\epsilon'b^2/t^2$ and w/b with b^2/Rt and b/R as parameters. The points are plotted solid for $\epsilon' \geq 0.003$. Data for panels 1, 2, and 10 were not plotted since these panels were tested without wire strain gages and the buckling was so sudden that the Tuckerman strain gages were thrown out of adjustment and the necessary reset had to be made by extrapolation. It was thought that this was not accurate enough for computing effective width.

Theoretical and empirical formulas for effective width
are also plotted in figures 32 to 36. These are Marguerre's
formula for the effective width of flat sheet with simply
supported edges (equation (14)), Wenzek's formula for curved
sheet (equation (15)), theoretical curves for a curved long
plate having simply supported edges (fig. 29), and theoret-
ical curves for a flat plate having clamped edges (reference
12).

Comparison of the observed effective widths with those
computed from the theoretical and empirical formulas shows
the observed effective widths to be somewhat higher except
for the flat panel 7 (fig. 32), which checks the theory of
reference 12 for flat plates having clamped edge support.
Effective widths at loads above the buckling load were ob-
tained only for panels 3, 4, 5, 6, 7, 8, 9, and 11. Of
these, panels 3 to 6 had sheet so thin that the restraint by
the stringers approached the clamped edge condition. This
may account for the measurement of effective widths well
above those given by Wenzek's formula, which holds for a
condition of restraint intermediate between simple and
clamped support at the edges. Panels 8 to 11 with sheet of
intermediate thickness gave effective widths that were only
a little above Wenzek's formula. All panels gave effective
widths larger than those computed from the theory of refer-
ence 1 which assumes simple edge support. At strains out-
side the plastic range ($\epsilon' > 0.003$), the effective widths
approached Marguerre's formula for flat sheet with simply
supported edges. (See equation (14).)

Buckling of panel as a whole between edge guides.- Pan-
els 17, 19, and 20, with a reinforcement ratio (area of
stringers/total area) between 0.178 and 0.193 failed by
buckling of the panel as a whole between edge guides. In
these panels the reinforcement was apparently not suffi-
ciently stiff to prevent lateral displacements of the sheet
at the stringers. Panels 18 and 21 did not fail by buckling
as a whole although they had the same reinforcement ratios
as panels 17 and 19. It appears from this that the critical
value of reinforcement ratio for which panels of this type,
with a width of 16 inches, may or may not fail by buckling
of the panel as a whole between edge guides is about 0.18.
The critical reinforcement ratio may be expected to increase
with increase of panel width and with decrease in curvature.
In the panels tested, however, the effects of differences in
curvature were less than the random variations due to other
causes.

No theoretical estimate of critical reinforcement ratio
was made since the only available method of analysis (reference 13, pp. 372 to 378) considers only up to two stringers
and only material which is elastic; whereas, panels 17 to 21
had four stringers each and failed in the plastic range.

Strength of panels.- The observed loads at failure are
plotted against computed loads in figure 37. The computed
loads were obtained from the nomogram for flat 24S-T
aluminum-alloy panels (fig. 56 of reference 4) assuming a
stringer stress at failure of 39 kips per square inch. This
value of stringer stress is an average for the flat panels
of reference 4, which had stringers of the same design as
those used in the curved panels.

Figure 37 shows that for 19 of the 21 panels tested,
covering a range of b^2/Rt from 0 to 32.6, the observed
loads differed from the calculated loads for similar flat
panels by not more than 6 percent. The remaining 2 panels,
20 and 21, were 9 and 15 percent stronger, respectively.

National Bureau of Standards,
      Washington, D. C., May 1944.

REFERENCES

1. Levy, Samuel: Large-Deflection Theory of Curved Sheet.
      NACA TN No. 895, 1943.

2. Paul, D. A., Howell, F. N., and Grieshaber, H. E.: Comparison of Stress-Strain Curves Obtained by the Single-Thickness and Pack Method. NACA TN No. 819, 1941.

3. Aitchison, C. S., and Tuckerman, L. B.: The "Pack" Method for Compressive Tests of Thin Specimens of Materials Used in Thin-Wall Structures. NACA Rep. No. 649, 1939.

4. Levy, Samuel, McPherson, Albert E., and Ramberg, Walter:
      Effect of Rivet and Spot-Weld Spacing on the Strength
      of Axially Loaded Sheet-Stringer Panels of 24S-T Aluminum Alloy. NACA TN No. 856, 1942.

5. Ramberg, Walter, McPherson, Albert E., and Levy, Sam:
   Compressive Tests of a Monocoque Box. NACA TN No. 721,
   1939.

6. Wenzek, W. A.: The Effective Width of Curved Sheet after
   Buckling. NACA TM No. 880, 1938.

7. Leggett, D. M. A.: The Buckling of a Long Curved Panel
   under Axial Compression. R. & M. No. 1899, British
   A.R.C., 1942.

8. Redshaw, S. C.: The Elastic Instability of a Thin Curved
   Panel Subjected to an Axial Thrust, its Axial and Cir-
   cumferential Edges Being Simply Supported. R. & M. No.
   1565, British A.R.C., 1934.

9. Stowell, Elbridge Z.: Critical Compressive Stress for
   Curved Sheet Supported along All Edges and Elastically
   Restrained against Rotation along the Unloaded Edges.
   NACA RB No. 3I07, 1943.

10. Howland, W. Lavern: Effect of Rivet Spacing on Stiffened
    Thin Sheet under Compression. Jour. Aero. Sci., vol.
    3, no. 12, Oct. 1936, pp. 434-439.

11. Ramberg, Walter, McPherson, Albert E., and Levy, Sam:
    Experimental Study of Deformation and of Effective
    Width in Axially Loaded Sheet-Stringer Panels. NACA
    TN No. 684, 1939.

12. Levy, Samuel, and Krupen, Philip: Large-Deflection The-
    ory for End Compression of Long Rectangular Plates
    Rigidly Clamped along Two Edges. NACA TN No. 884,
    1943.

13. Timoshenko, S.: Theory of Elastic Stability. McGraw-
    Hill Book Co., Inc. (New York), 1936.

14. Lundquist, Eugene E., and Schuette, Evan H.: Critical
    Stresses for Plates. NACA ARR No. 3J27, 1943.

TABLE 1.- DIMENSIONS OF PANELS
[See also fig. 1.]

Panel	Radius, R (in.)	Cross-sectional area of panel (sq in.)	Average cross-sectional area of a stringer (sq in.)	Length of panel, l (in.)	Developed width of panel, 4b (in.)	Thickness of sheet, t (in.)	Rivet spacing, L (in.)	$\frac{b}{t}$	$\frac{L}{t}$	$\frac{b^2}{Rt}$
1	76.5	1.167	0.193	11.97	16.00	0.0247	0.50	162	20.2	8.47
2	38.2	1.103	.171	11.95	16.00	.0260	.50	154	19.2	16.1
3	25.5	1.077	.169	11.93	16.00	.0251	.50	159	19.9	25.0
4	19.1	1.114	.176	11.96	16.00	.0257	.50	156	19.4	32.6
5	19.1	1.101	.174	11.98	16.00	.0257	1.00	156	38.9	32.6
6	19.1	1.120	.177	11.97	16.00	.0257	2.00	156	77.8	32.6
7	∞	1.537	.179	11.95	16.00	.0512	1.00	78.1	19.5	0
8	76.5	1.551	.177	11.97	16.00	.0527	1.00	75.9	19.0	3.97
9	38.2	1.536	.175	11.93	16.00	.0523	1.00	76.5	19.1	8.01
10	25.5	1.507	.169	11.96	16.00	.0519	1.00	77.1	19.3	12.1
11	19.1	1.519	.171	11.97	16.00	.0522	1.00	76.6	19.2	16.0
12	∞	2.280	.172	11.98	16.00	.0996	1.50	40.1	15.1	0
13	76.5	2.336	.189	11.97	16.00	.0987	1.50	40.5	15.2	2.19
14	38.2	2.298	.177	11.98	16.00	.0994	1.50	40.3	15.1	4.16
15	25.5	2.307	.180	11.97	16.00	.0991	1.50	40.4	15.1	6.33
16	19.1	2.269	.172	11.95	16.00	.0987	1.50	40.5	15.2	8.26
17	∞	3.719	.179	11.98	16.00	.1873	1.50	21.4	8.0	0
18	75.9	3.705	.179	11.96	16.00	.1872	1.50	21.4	8.0	1.12
19	38.2	3.663	.163	11.97	16.07	.1875	1.50	21.4	8.0	2.23
20	25.5	3.685	.168	11.94	16.08	.1876	1.50	21.4	8.0	3.34
21	19.1	3.721	.166	11.94	16.10	.1899	1.50	21.2	7.9	4.41

TABLE 2.- TENSILE AND COMPRESSIVE PROPERTIES OF SHEET
[See also fig. 2]

Nominal thickness of sheet (in.)	Direction of load	Young's modulus		Yield strength (0.002 offset)		Tensile strength
		Tension (kips/sq in.)	Compression (kips/sq in.)	Tension (kips/sq in.)	Compression (kips/sq in.)	(kips/sq in.)
0.025	Longitudinal	10,500	10,700	48.3	42.0	65.2
.025	Transverse	10,600	------------	44.1	------------	65.7
.051	Longitudinal	10,400	10,700	58.4	49.1	74.0
.051	Transverse	10,400	------------	49.6	------------	72.4
.100	Longitudinal	10,400	10,500	58.5	47.5	73.7
.100	Transverse	10,300	------------	49.2	------------	71.5
.188	Longitudinal	10,400	10,500	54.5	44.8	72.0
.188	Transverse	10,500	------------	47.0	------------	69.0

TABLE 3.- STRAINS AT FIRST OBSERVED BUCKLING

OF SHEET AND INSTABILITY OF STRINGERS

Panel	Buckling of sheet between stringers		Buckling of sheet between rivets	Instability of stringer	Buckling of panel as a whole between edge guides
	Part way between stringers	Stringer to stringer			
1	(2)	4.4×10^{-4}	(2)	[1] 50×10^{-4}	(2)
2	(2)	6.5	(2)	[1] 50	(2)
3	(2)	7.7	[1] 45×10^{-4}	[1] 45	(2)
4	(2)	10.1	[1] 45	[1] 45	(2)
5	9.5×10^{-4}	10.0	33	[1] 45	(2)
6	(2)	8.7	10.1	[1] 45	(2)
7	(2)	8.2	39	40	(2)
8	(2)	9.3	[1] 45	[1] 50	(2)
9	(2)	14.5	[1] 43	[1] 43	(2)
10	(2)	16.0	[1] 44	[1] 47	(2)
11	23	[1] 50	[1] 40	[1] 38	(2)
12	(2)	26.0	[1] 30	(2)	(2)
13	(2)	28.0	[1] 34	(2)	(2)
14	(2)	32	(2)	[1] 40	(2)
15	(2)	31	[1] 32	[1] 35	(2)
16	(2)	34	(2)	[1] 34	(2)
17	(2)	(2)	(2)	(2)	[1] 45
18	(2)	(2)	(2)	[1] 35	(2)
19	(2)	(2)	(2)	(2)	[1] 50
20	(2)	38.3	(2)	31	41
21	(2)	[1] 33	(2)	[1] 44	(2)

[1] Estimated from observed data.

[2] No buckling observed at any load.

TABLE 4.- FAILURE OF PANELS

Panel	Maximum load, P (kips)	Average stress, P/A (kips/sq in.)	Average stringer stress, σ_{st} (extrapolated) (kips/sq in.)	Average sheet strain (extrapolated)	Type of failure
1	36.2	31.0	40.0	0.0059	Stringer instability[1]
2	32.8	29.7	37.0	.0050	Do.
3	32.3	30.0	37.2	.0048	Do.
4	33.2	29.8	37.5	.0046	Do.
5	30.2	27.4	36.2	.0048	Do.
6	30.2	27.0	36.4	.0049	Do.
7	44.9	29.2	35.8	.0042	Do.
8	44.8	28.9	35.8	.0050	Do.
9	44.5	29.0	37.2	.0045	Do.
10	42.5	28.2	36.2	.0047	Do.
11	44.2	29.1	34.3	.0038	Do.
12	74.8	32.8	37.9	.0036	Rivet separation
13	76.9	32.9	33.4	.0038	Do.
14	76.1	33.1	31.4	.0040	Stringer instability[1]
15	80.0	34.7	33.2	.0035	Do.
16	81.8	36.1	34.6	.0038	Buckling of sheet[2]
17	138.4	37.2	36.0	.0045	Buckling of panel[3]
18	135.0	36.4	40.0	.0042	Stringer instability[1]
19	143.5	39.2	39.4	.0050	Buckling of panel[3]
20	149.9	40.7	38.3	.0048	Do.[3]
21	158.1	42.5	40.0	.0060	Stringer instability[1]

[1] Stringers failed by twisting.

[2] Sheet buckled between stringers at maximum load.

[3] Buckling of panel as a whole between edge guides.
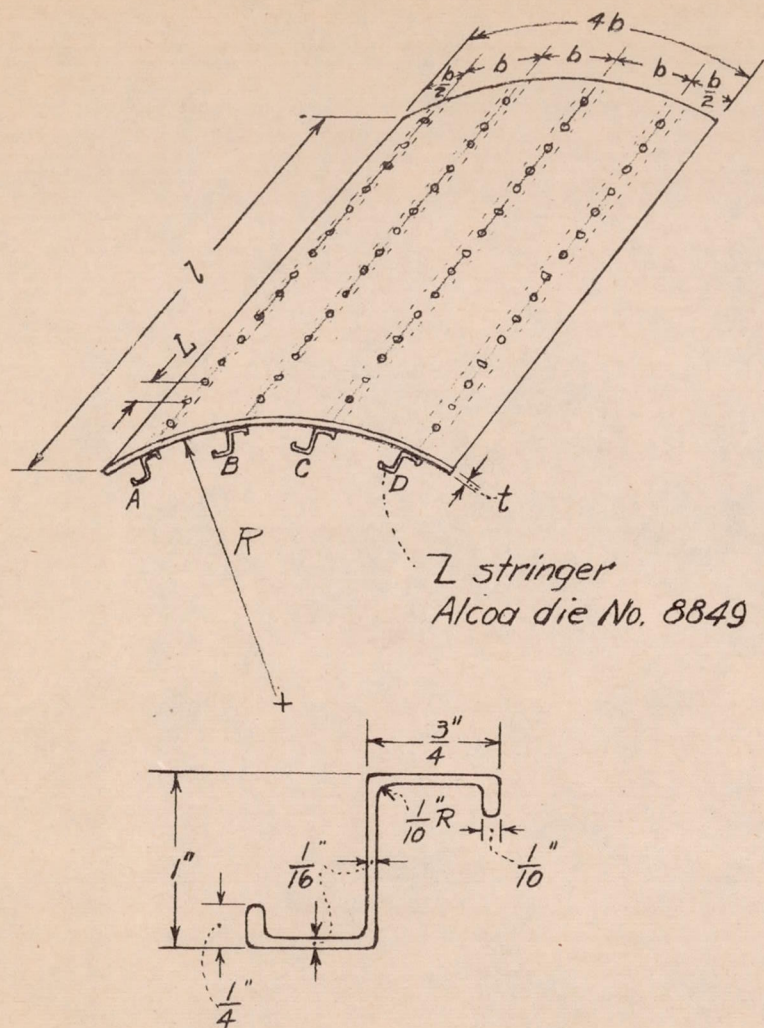
Figure 1.- Construction of sheet-stringer panels and nominal dimensions of stringer. Stringers fastened to sheet by 1/8-inch brazier-head rivets. All material 24S-T aluminum alloy.
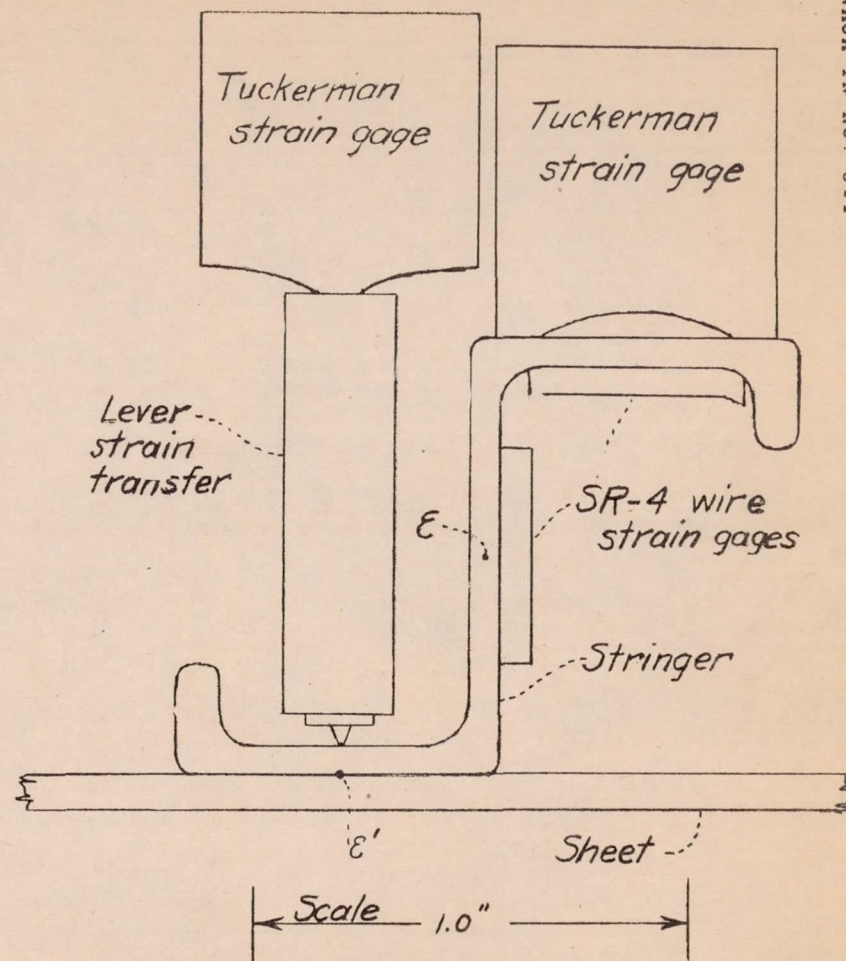
Figure 5.- Location of strain gages on stringer cross-section.
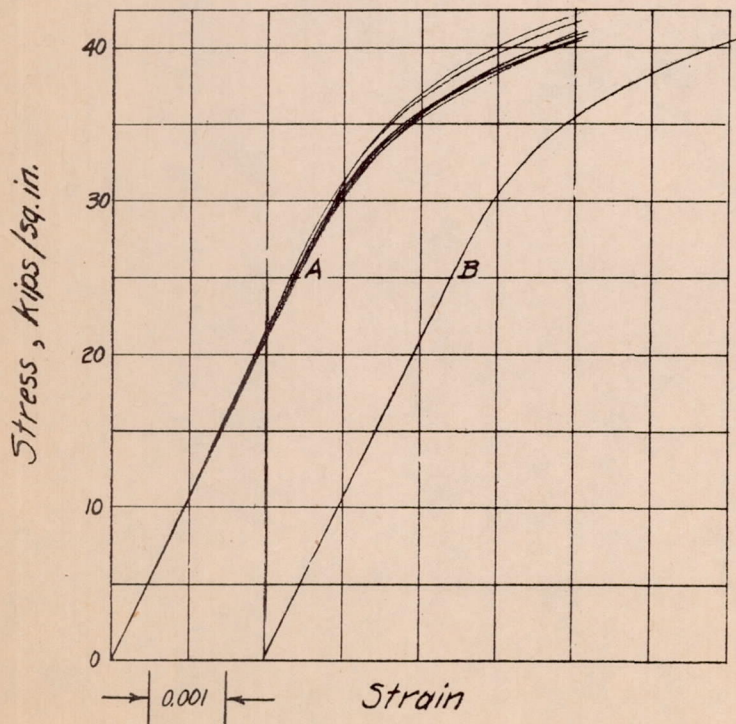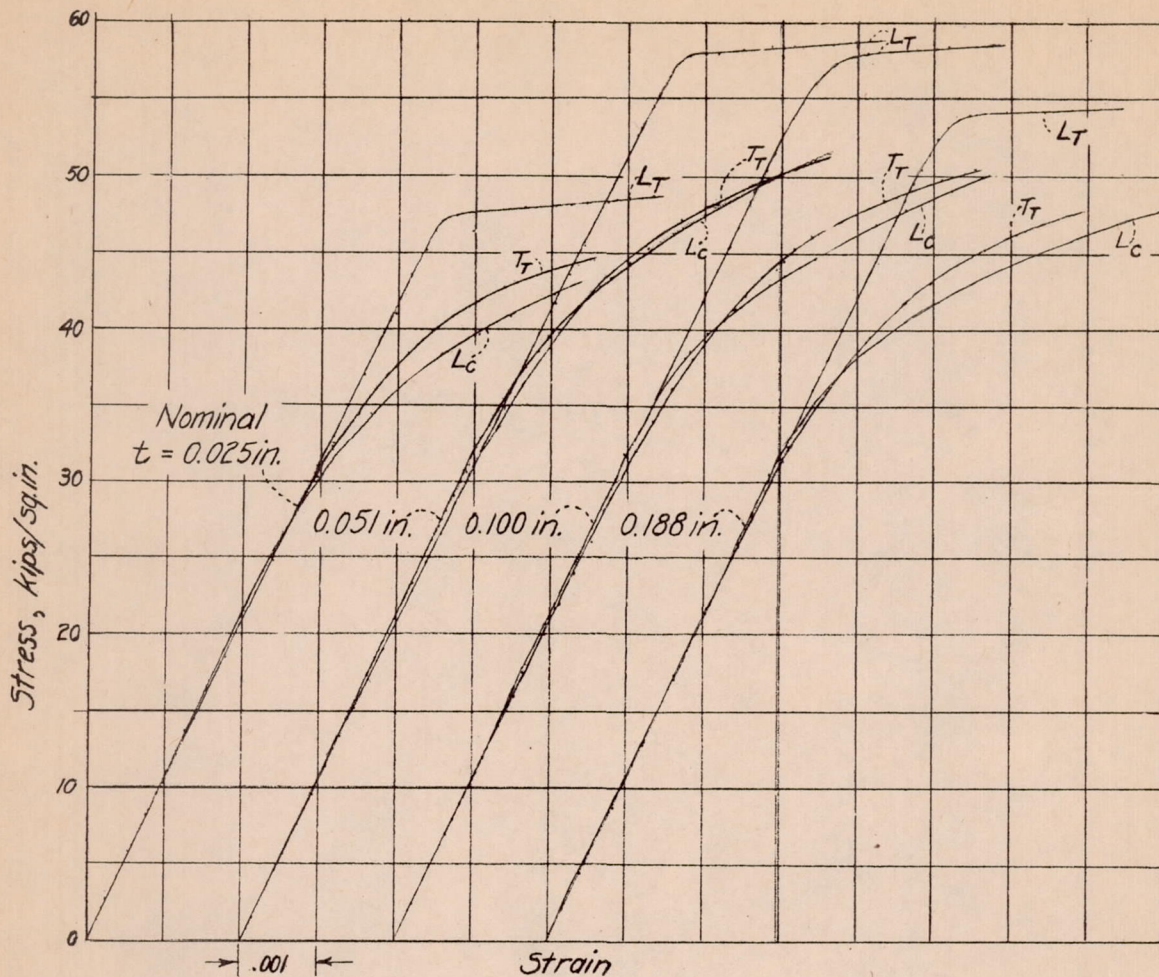
Figure 2.- Stress-strain curves of 24S-T aluminum alloy sheet used in panels. L_T, tension in direction of rolling; L_C, compression in direction of rolling; T_T, tension transverse to direction of rolling.

Figure 3.- Compressive stress-strain curves of four-inch lengths of Z-stringers; A, family of stress-strain curves for all the stringers; B, stress-strain curve used in computations for all panels.

Fig. 4
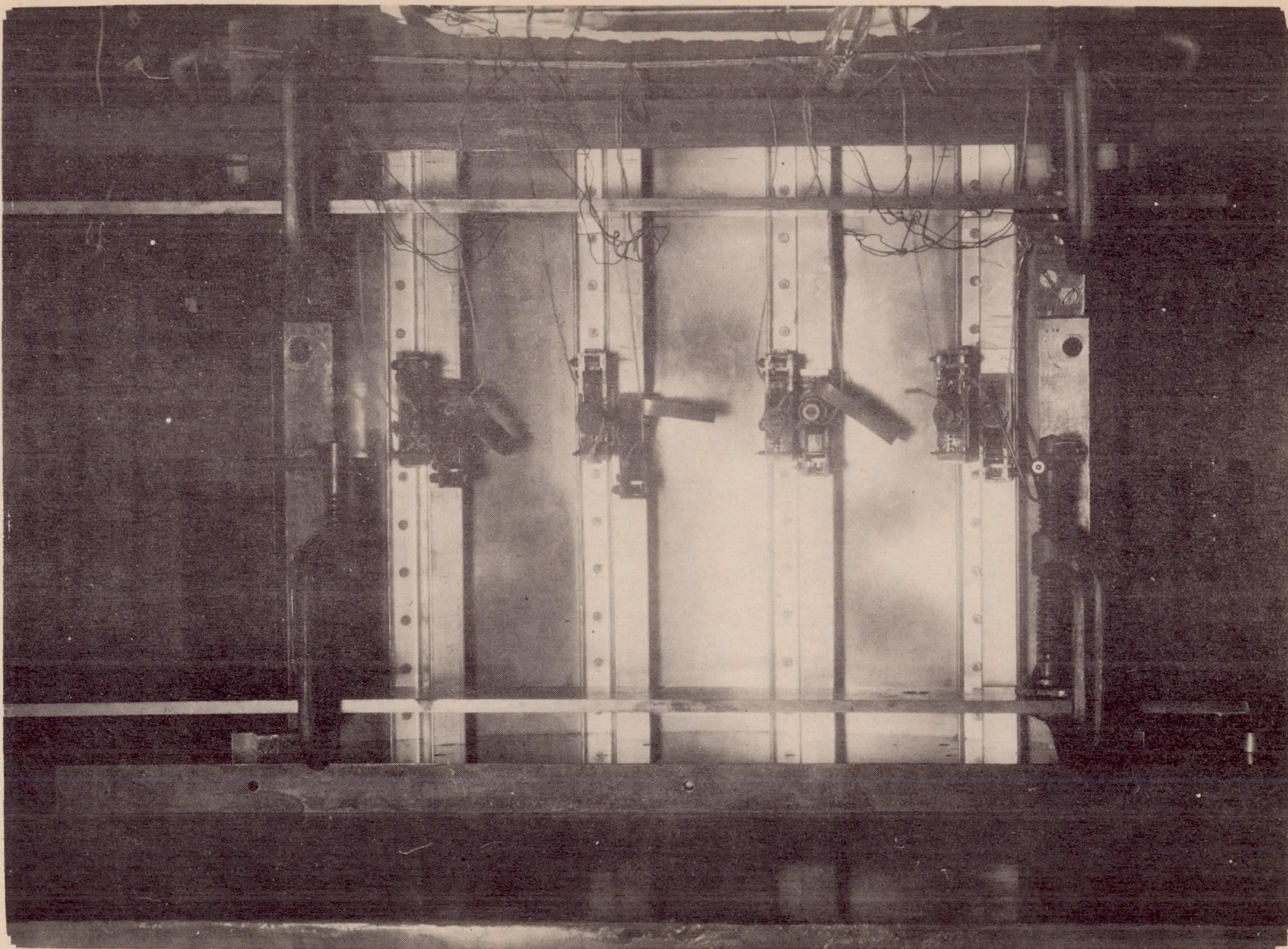
Figure 4.- Panel during test showing attachment of strain gages.
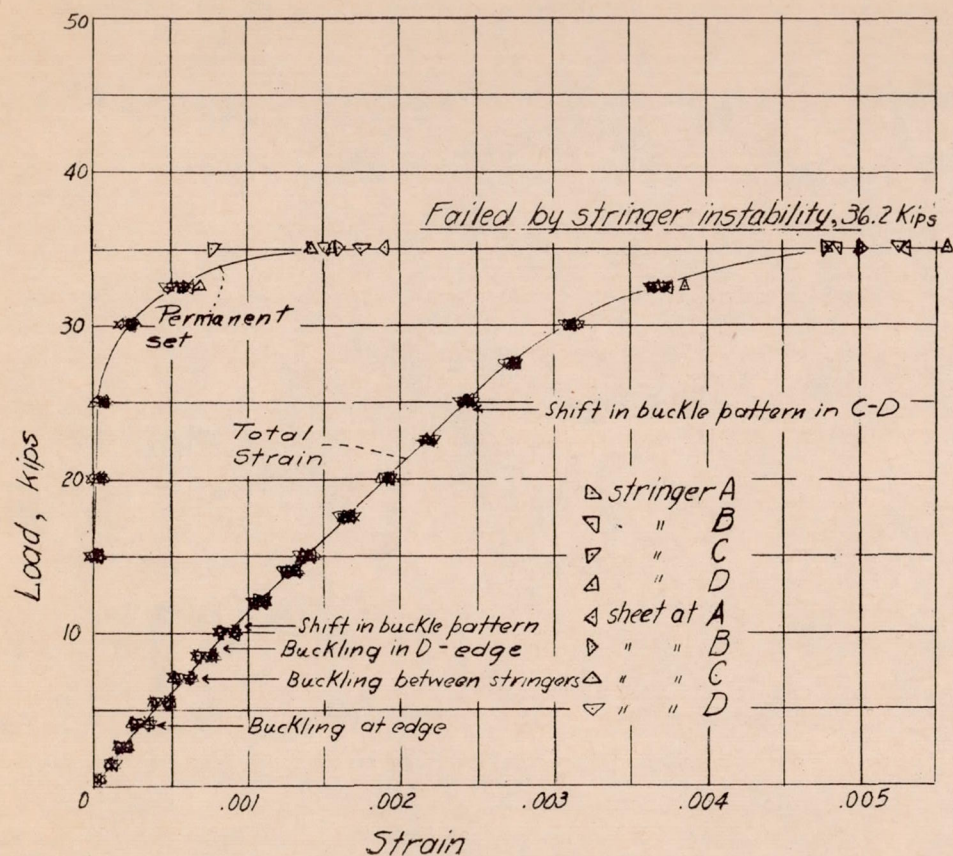
Figure 6.- Test of panel 1; radius, 76.5 inches.
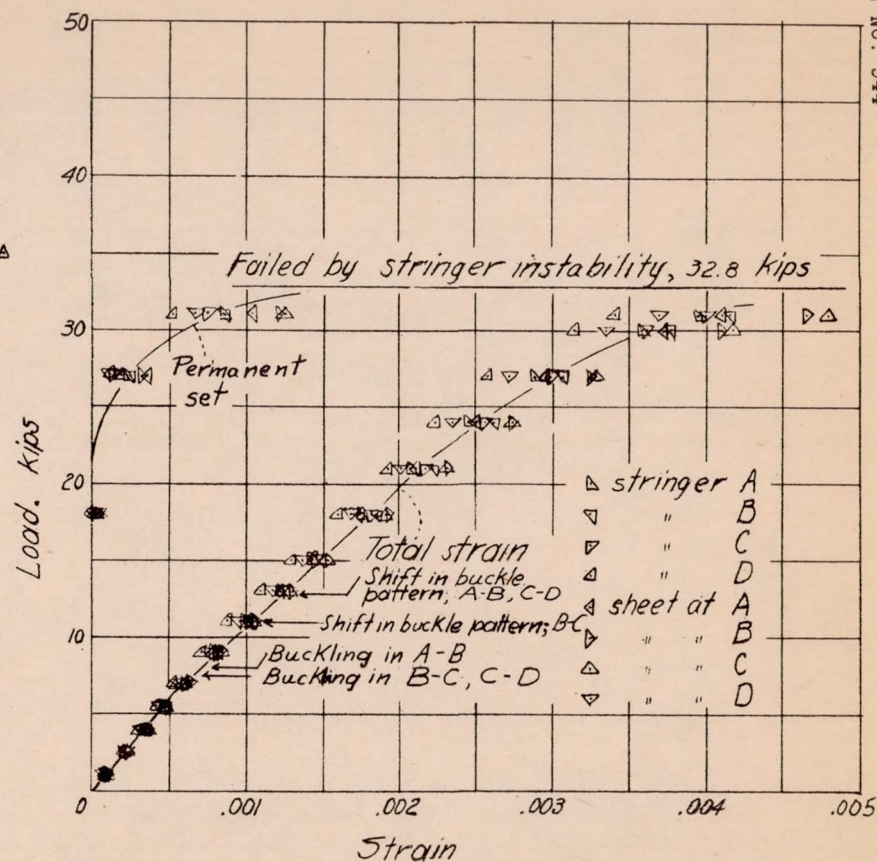
Figure 7.- Test of panel 2; radius, 38.2 inches.
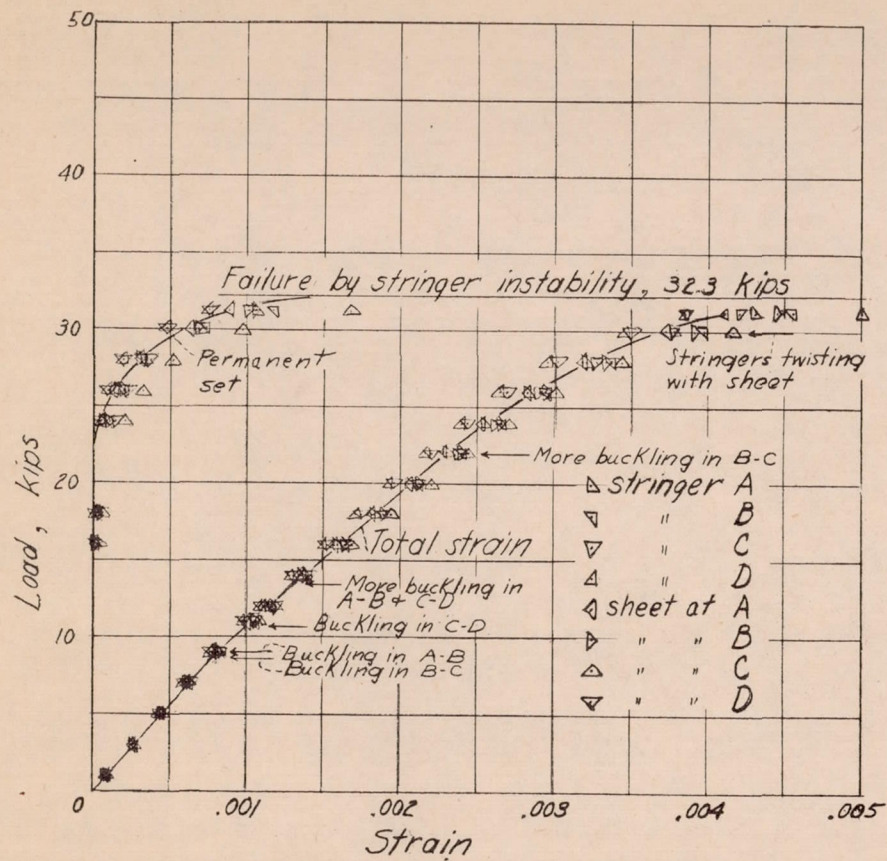
Figure 8.- Test of panel 3; radius, 25.5 inches.
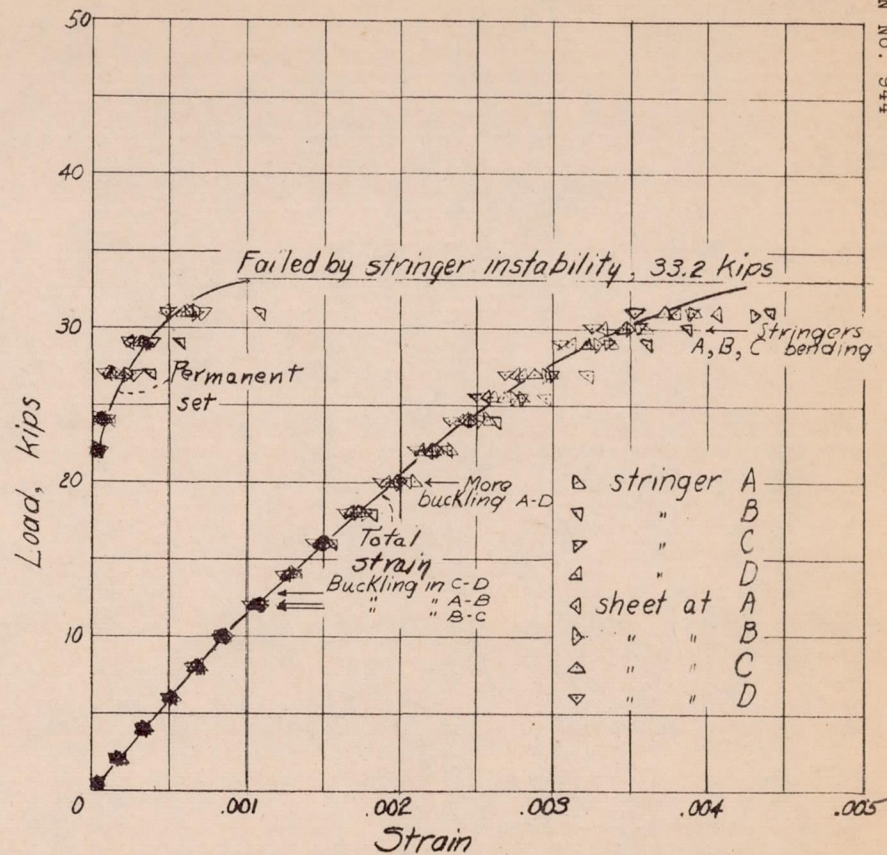
Figure 9.- Test of panel 4; radius, 19.1 inches.
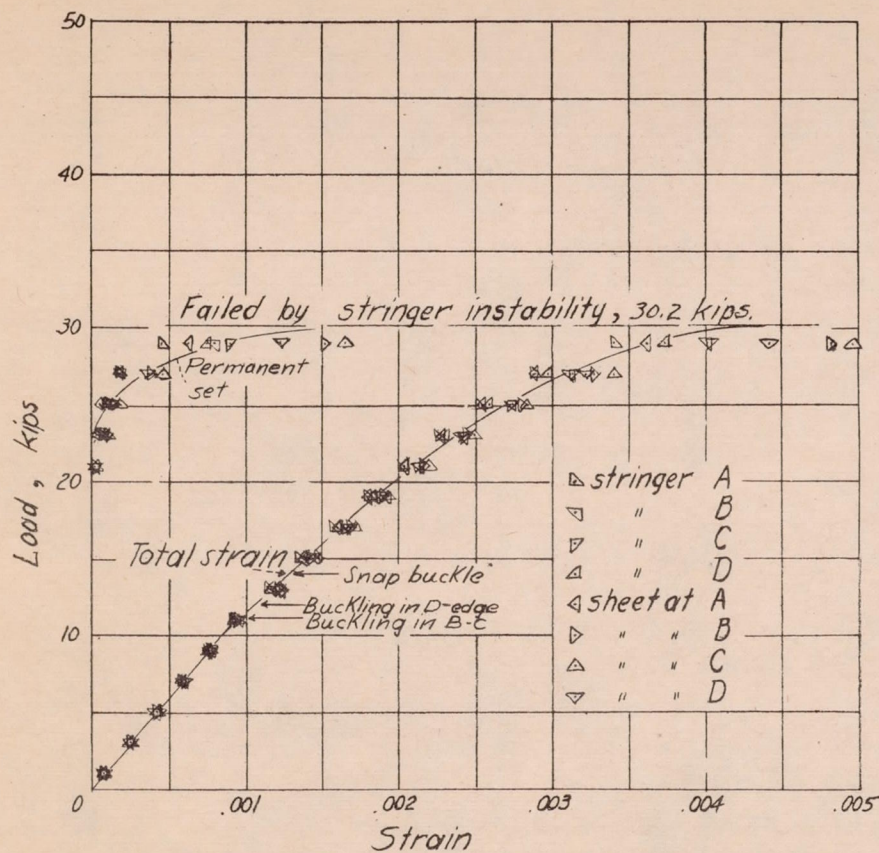
Figure 10.- Test of panel 5; radius, 19.1 inches.
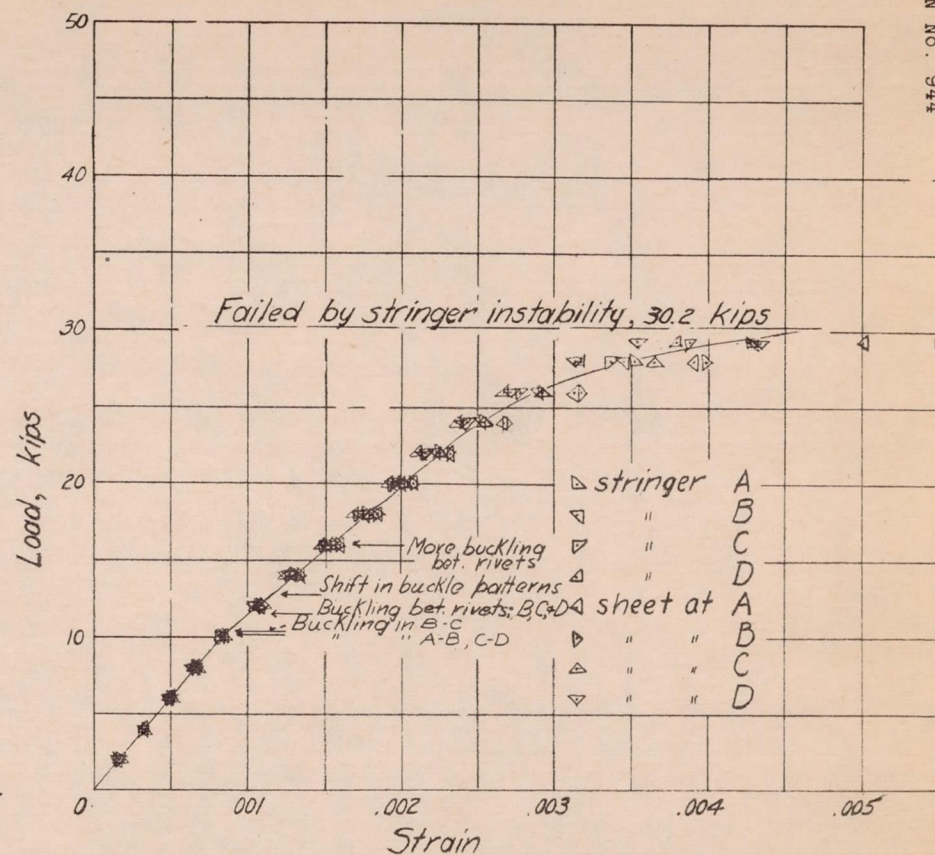

Figure 11.- Test of panel 6; radius, 19.1 inches.
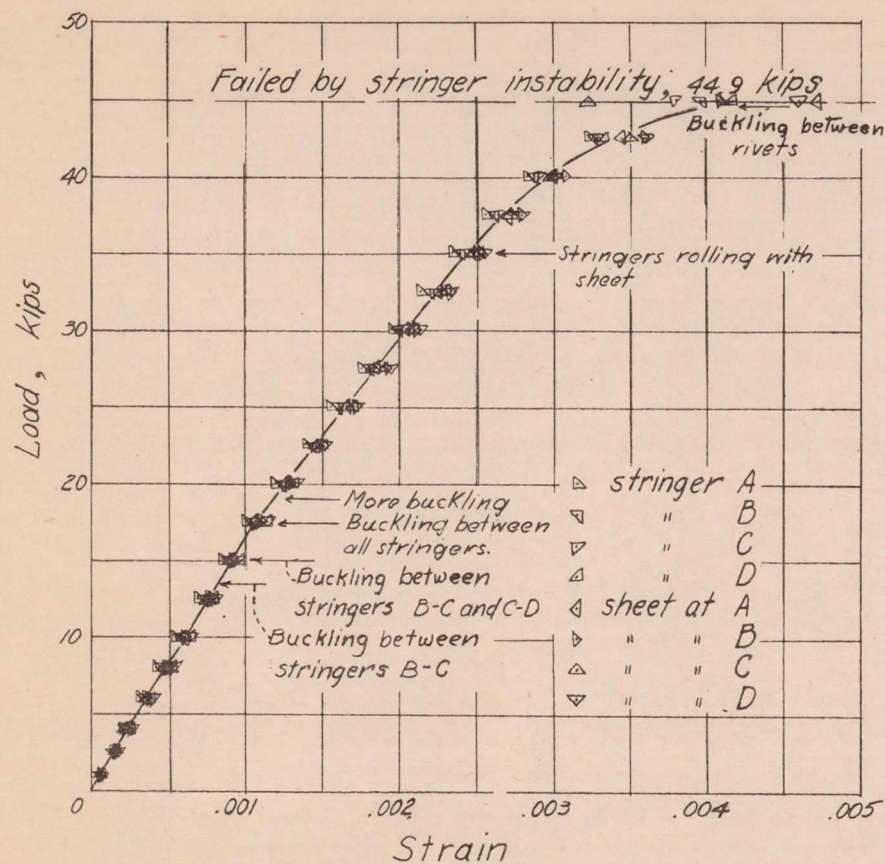
Figure 12.- Test of panel 7; flat sheet, (SR-4 gages used after 42.5 kips).
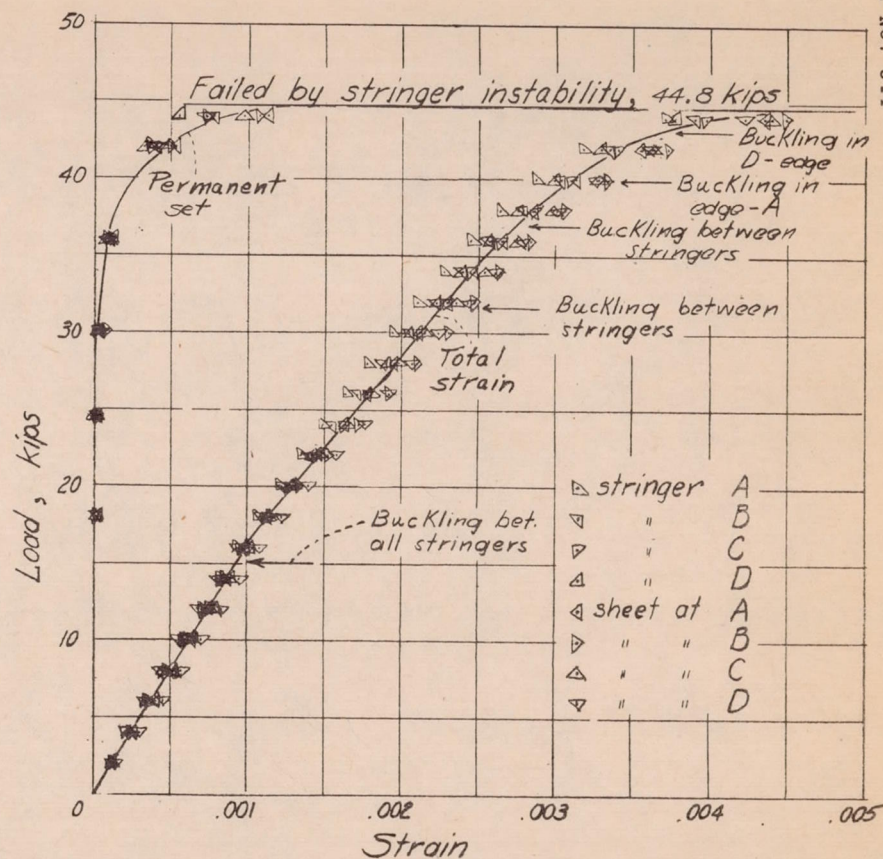
Figure 13.- Test of panel 8; radius, 76.5 inches.
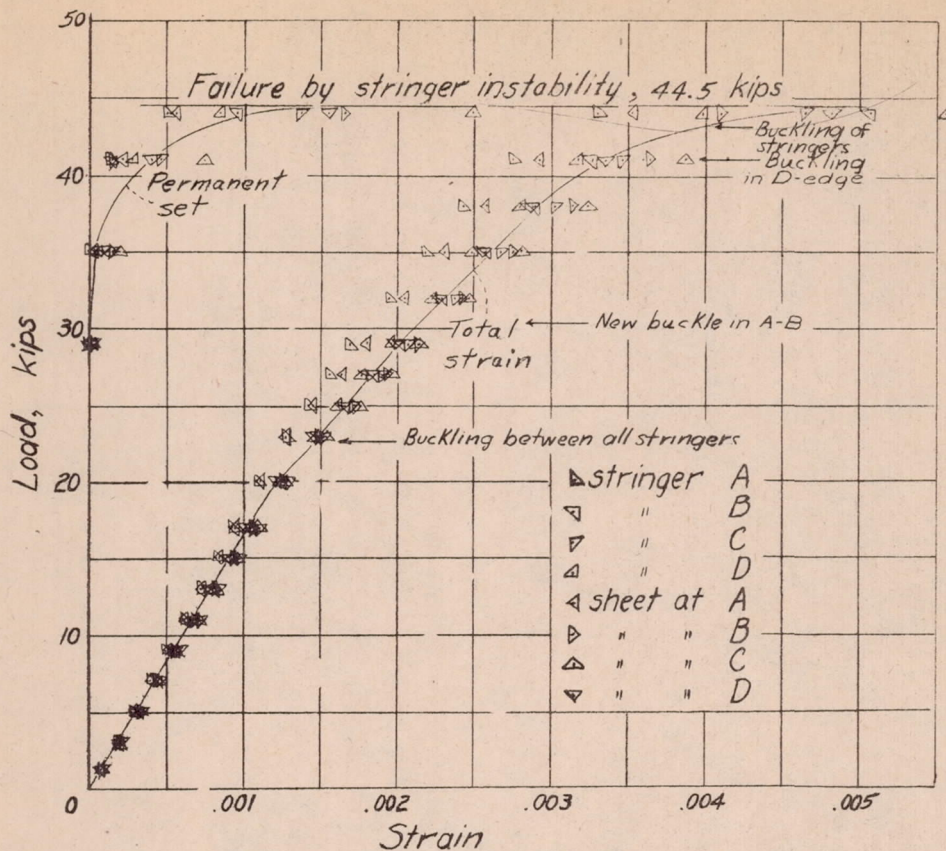
Figure 14.- Test of panel 9; radius, 38.2 inches.
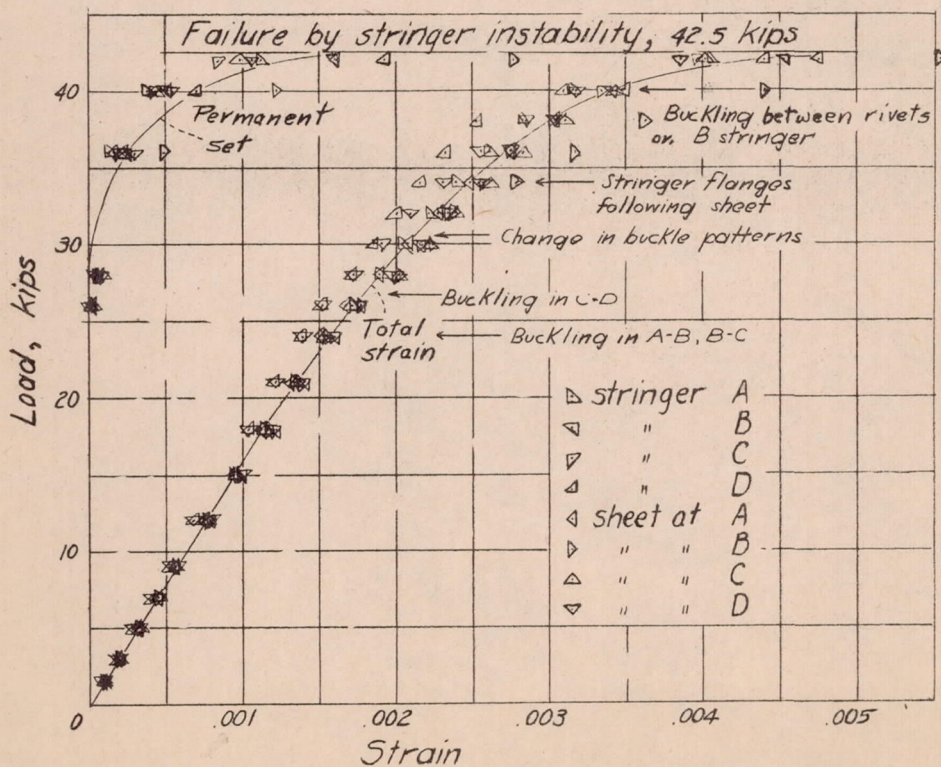
Figure 15.- Test of panel 10; radius, 25.5 inches.
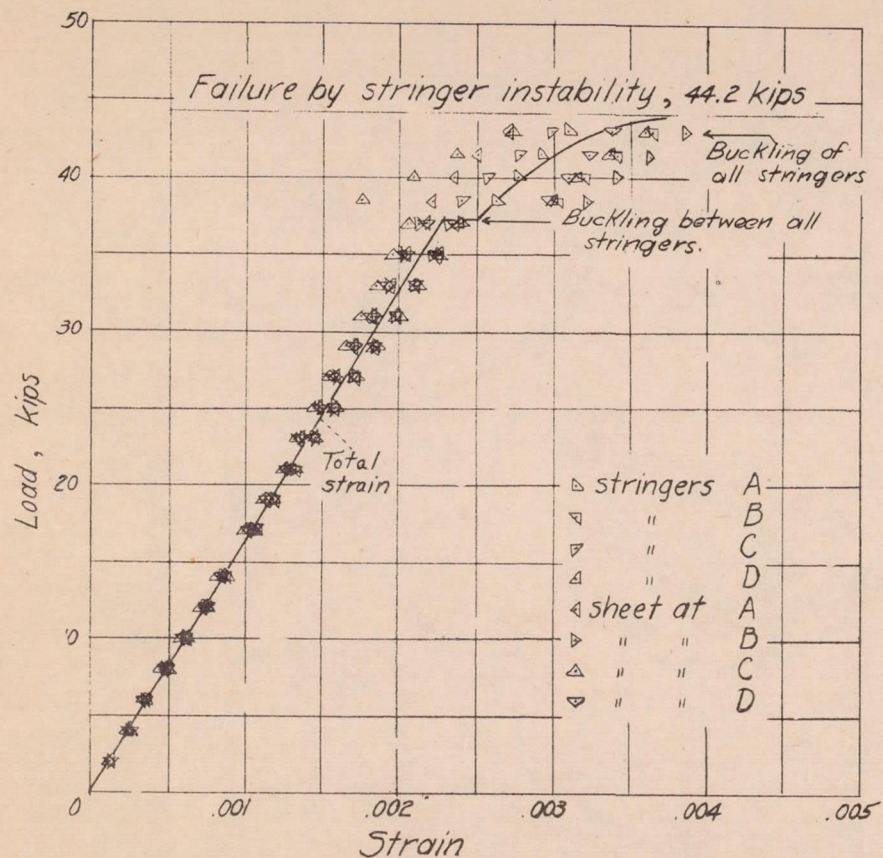
Figure 16.- Test of panel 11; radius, 19.1 inches, (SR-4 gages used to reset Tuckerman gages after buckling at 37.1 kips).
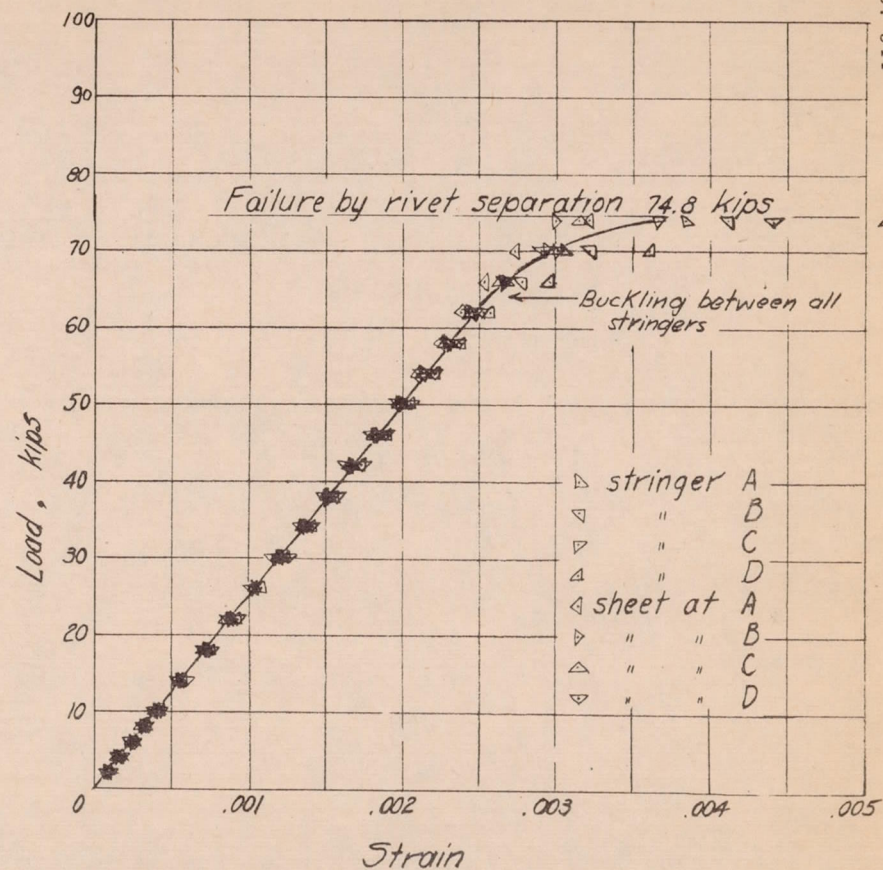
Figure 17.- Test of panel 12; flat sheet, (SR-4 gages used after 70.0 kips).

Failure by rivet separation, 76.9 kips

Stringers following sheet

Buckling between all stringers

stringer A
" B
" C
" D
sheet at A
" " B
" " C
" " D

Load, kips

Strain
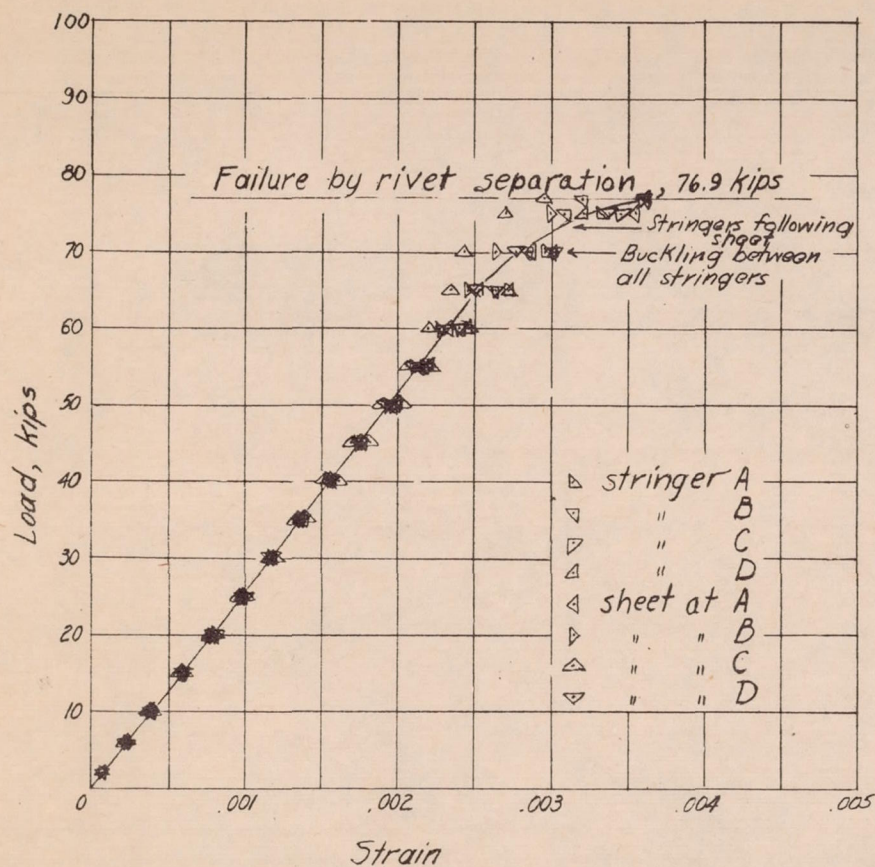
Figure 18.- Test of panel 13; radius, 76.5 inches.

Failure by stringer instability, 76.1 kips

Buckling in B-C

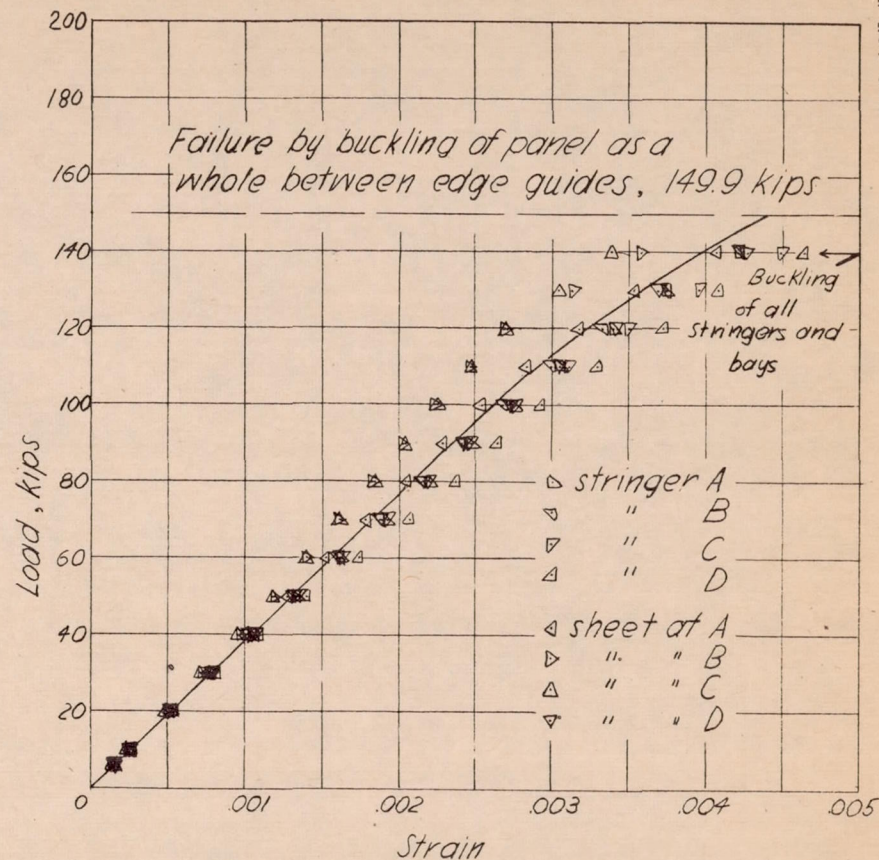stringer A
" B
" C
" D
sheet at A
" " B
" " C
" " D

Load, kips

Strain
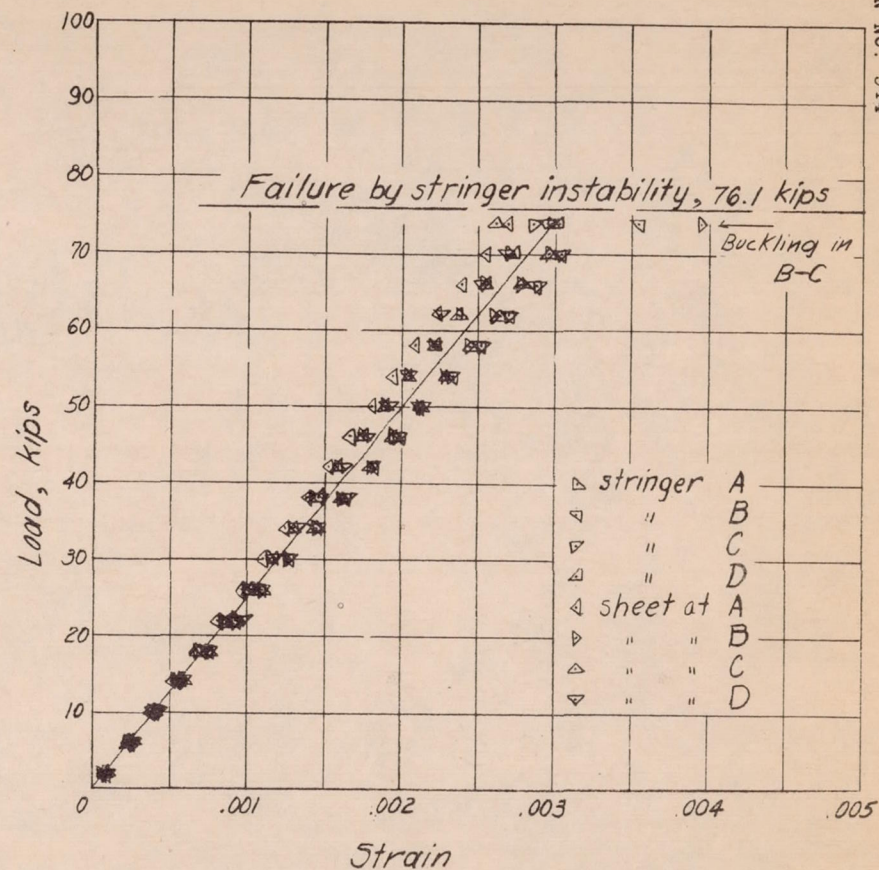
Figure 19.- Test of panel 14; radius, 36.5 inches.
(SR-4 gages used after 70.0 kips).
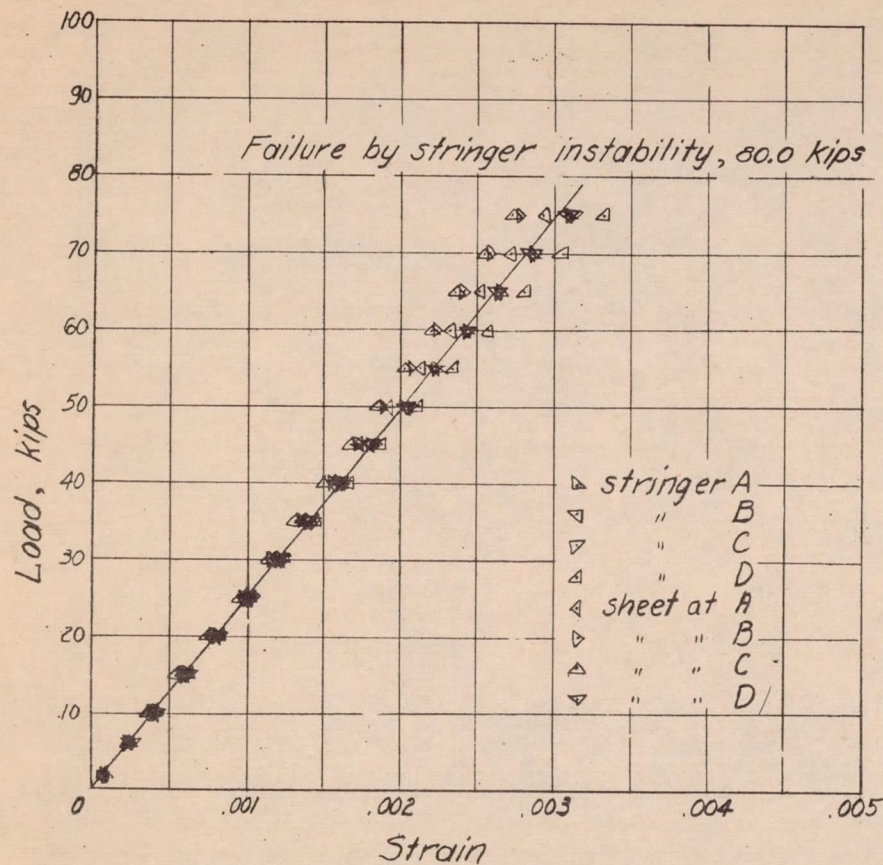
Figure 20.- Test of panel 15; radius, 25.5 inches.

Failure by stringer instability, 80.0 kips

stringer A
"   B
"   C
"   D
sheet at A
"   "   B
"   "   C
"   "   D
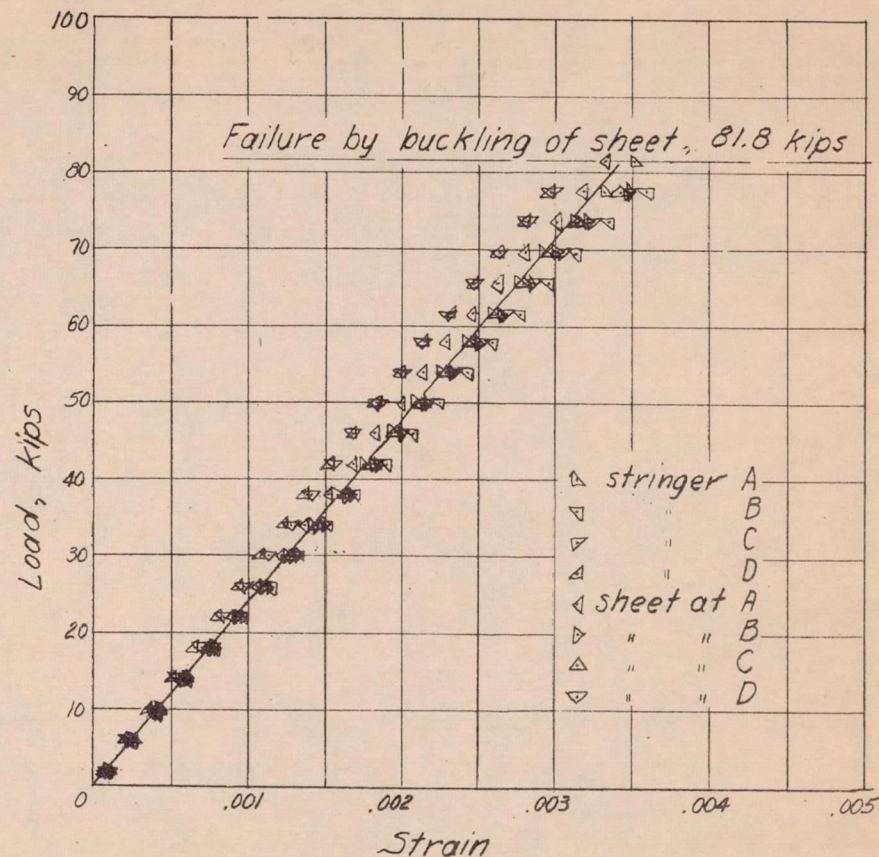
Figure 21.- Test of panel 16; radius, 19.1 inches.
(SR-4 gages used after 73.8 kips).

Failure by buckling of sheet, 81.8 kips

stringer A
"   B
"   C
"   D
sheet at A
"   "   B
"   "   C
"   "   D
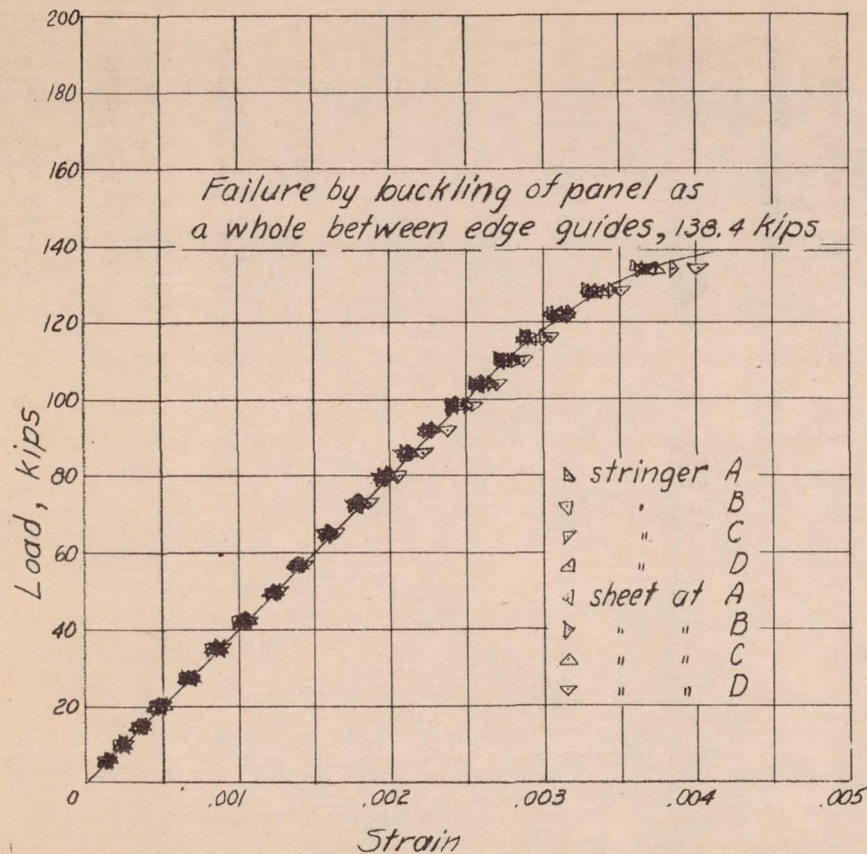
Figure 22.- Test of panel 17; flat sheet, (SR-4 gages used after 116 kips).
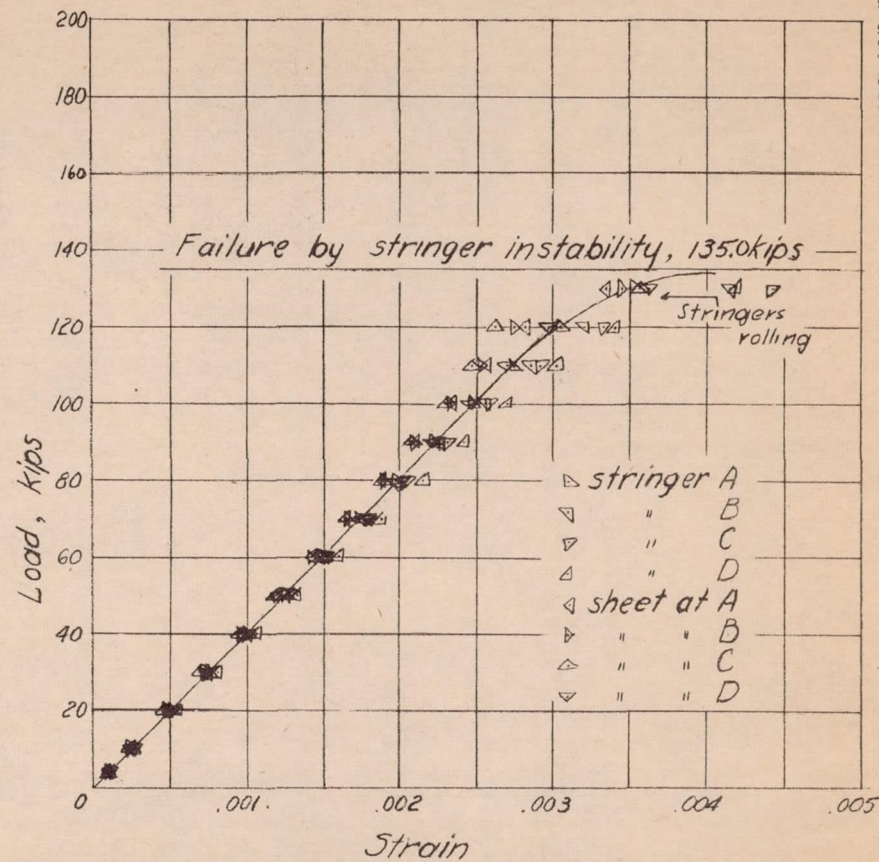
Figure 23.- Test of panel 18; radius, 75.9 inches. (SR-4 gages used after 120 kips).
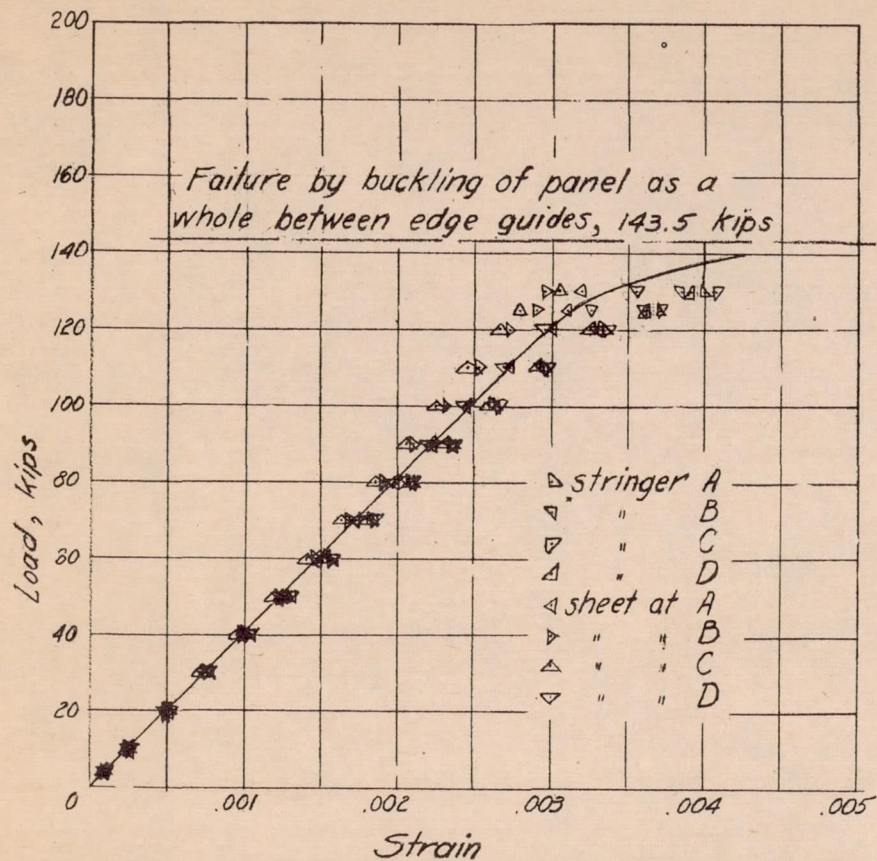
Figure 24.- Test of panel 19; radius, 36.5 inches,
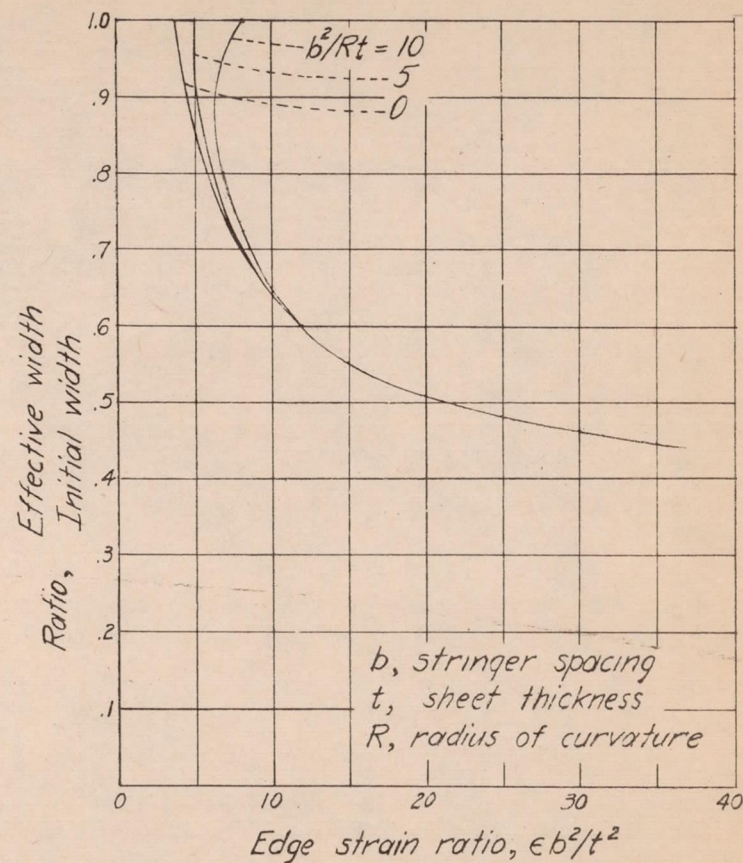(SR-4 gages used after 120 kips).

Figure 25.- Test of panel 20; radius, 25.5 inches.
(SR-4 gages used after 120 kips).

Failure by stringer instability, 158.1 kips

Buckling
of stringer D

▷ stringer A
▽ " B
▽ " C
△ " D
◁ sheet at A
▷ " " B
△ " " C
▽ " " D

Load, kips

Strain
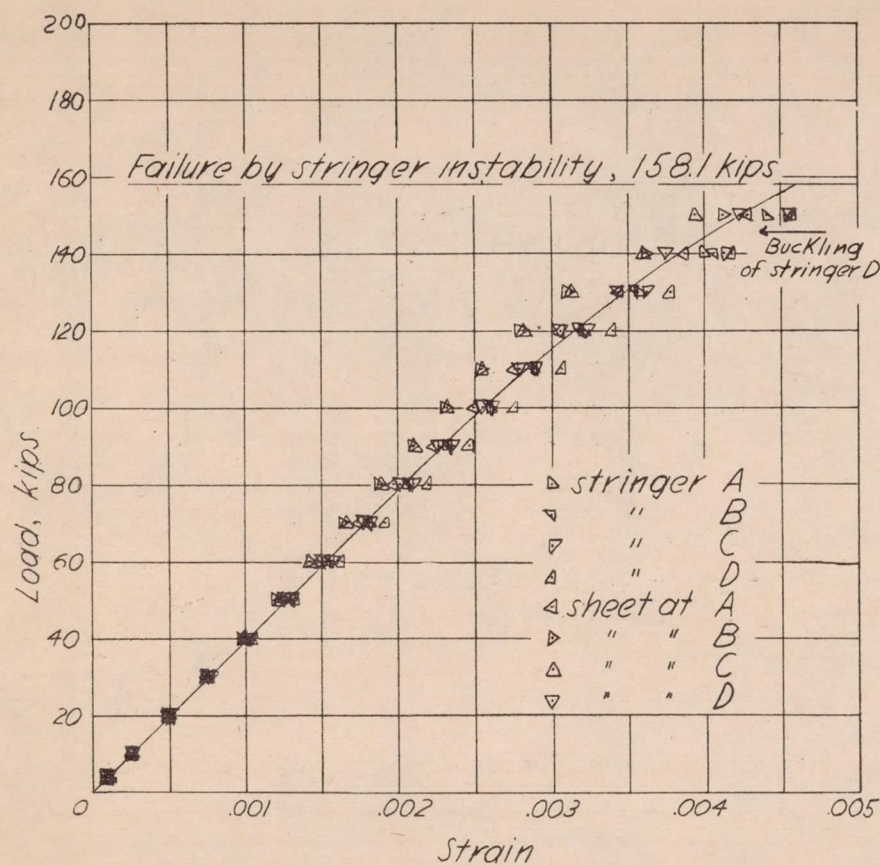
Figure 26.- Test of panel 21; radius 19.1 inches.
(SR-4 gages used after 130 kips).

$b^2/Rt = 10$
5
0

Ratio, $\dfrac{\text{Effective width}}{\text{Initial width}}$

b, stringer spacing
t, sheet thickness
R, radius of curvature

Edge strain ratio, $\epsilon b^2/t^2$

Figure 29.- Effective width ratio for long panel, simply-
supported on the edge (reference 1).
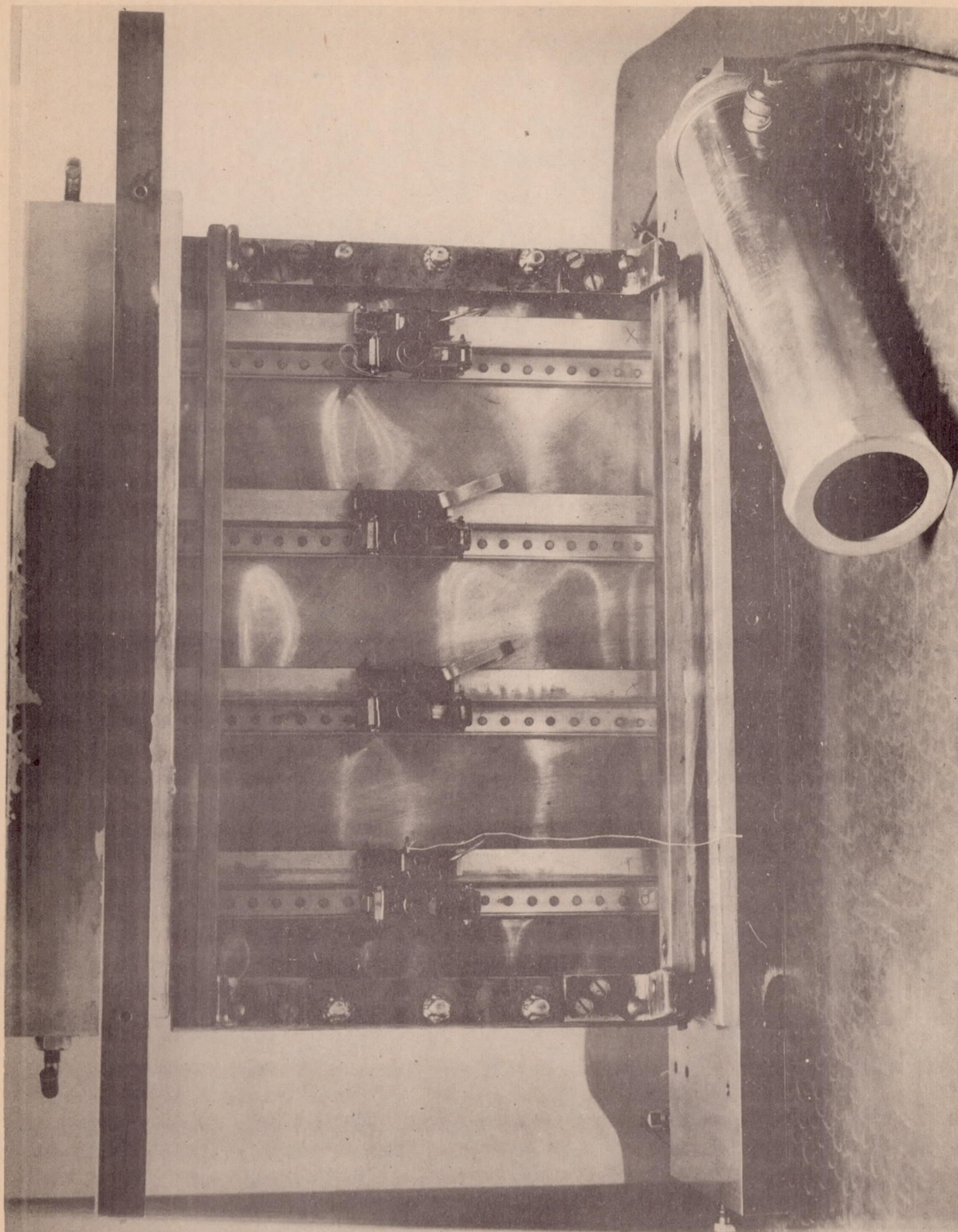
Figure 27.- Panel 1 at a load of 30.0 kips (stringer side).

Fig. 28
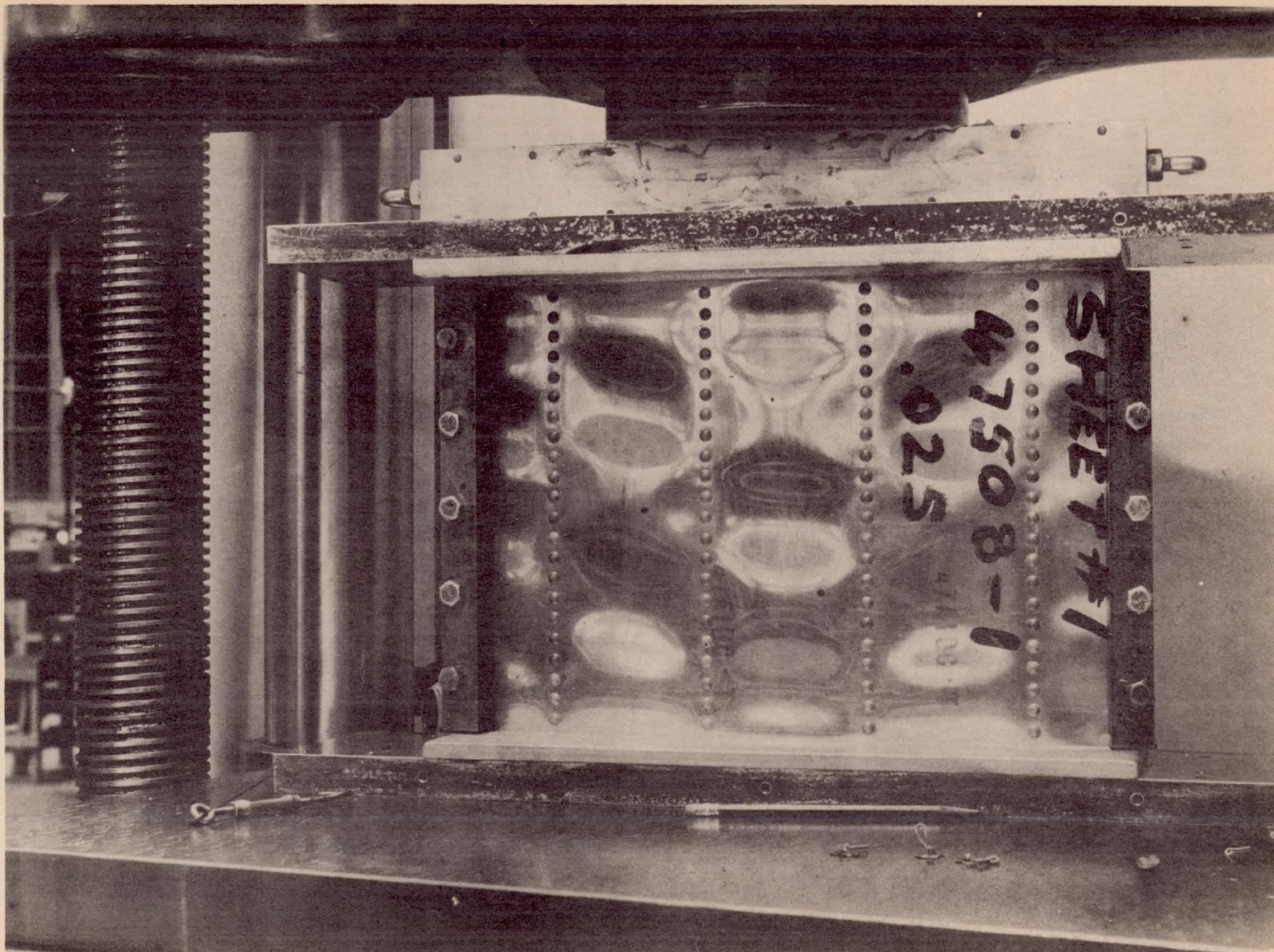
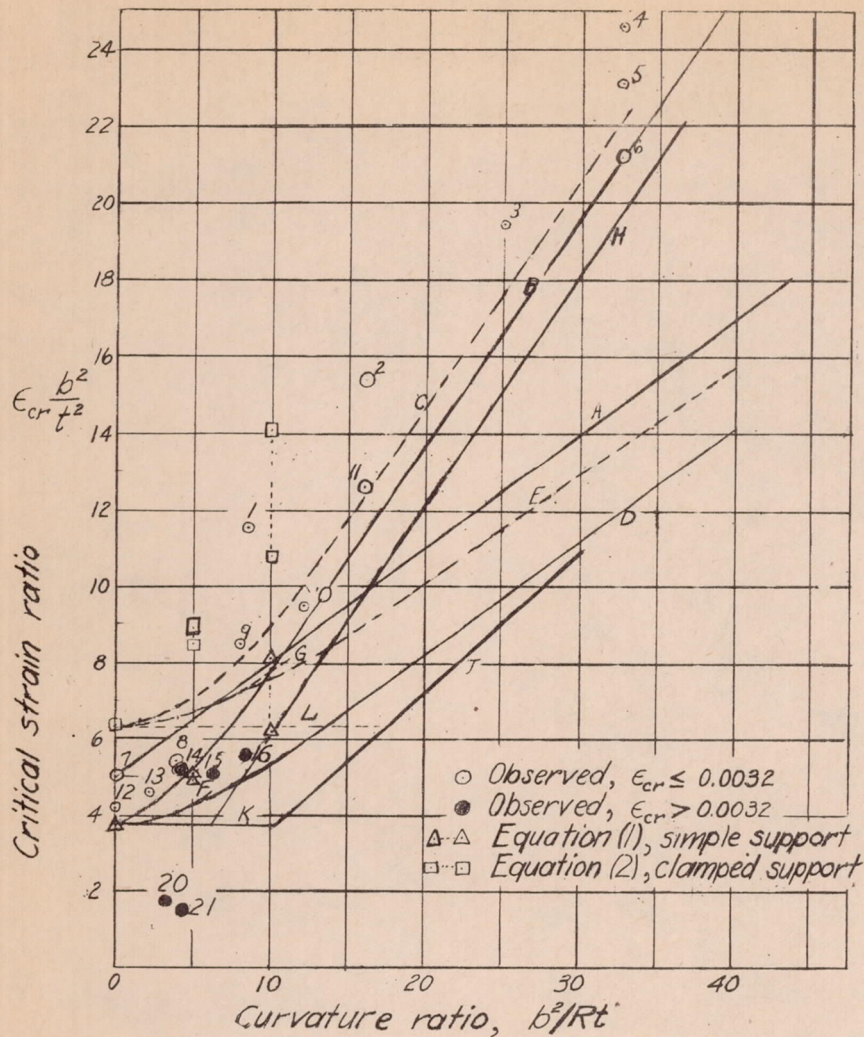Figure 28.- Sheet side of panel 1 at 30.0 kips showing buckle pattern.

Figure 30.- Critical strain for buckling of curved sheet between stringers; b = stringer spacing; t = sheet thickness; R = radius of curvature; ϵ_{cr} = strain for buckling between stringers.
Curve A - Eq.4, Wenzek
Curve B - Leggett. simple- support at stringers
Curve C - Leggett, clamping at stringers
Curve D - Eq.6, Stowell, simple-support at stringers, b^2/Rt large
Curve E - Eq.7, Stowell, clamping at stringers, b^2/Rt large
Curve F - Eq.9, Stowell, simple-support at stringers, b^2/Rt small
Curve G - Eq.10, Stowell, clamping at stringers, b^2/Rt small
Curve H - Eq.11a,
Curve J - Eq.11b,
Curve K - Eq.12a, simple support at stringers
Curve L - Eq.12b, clamping at stringers
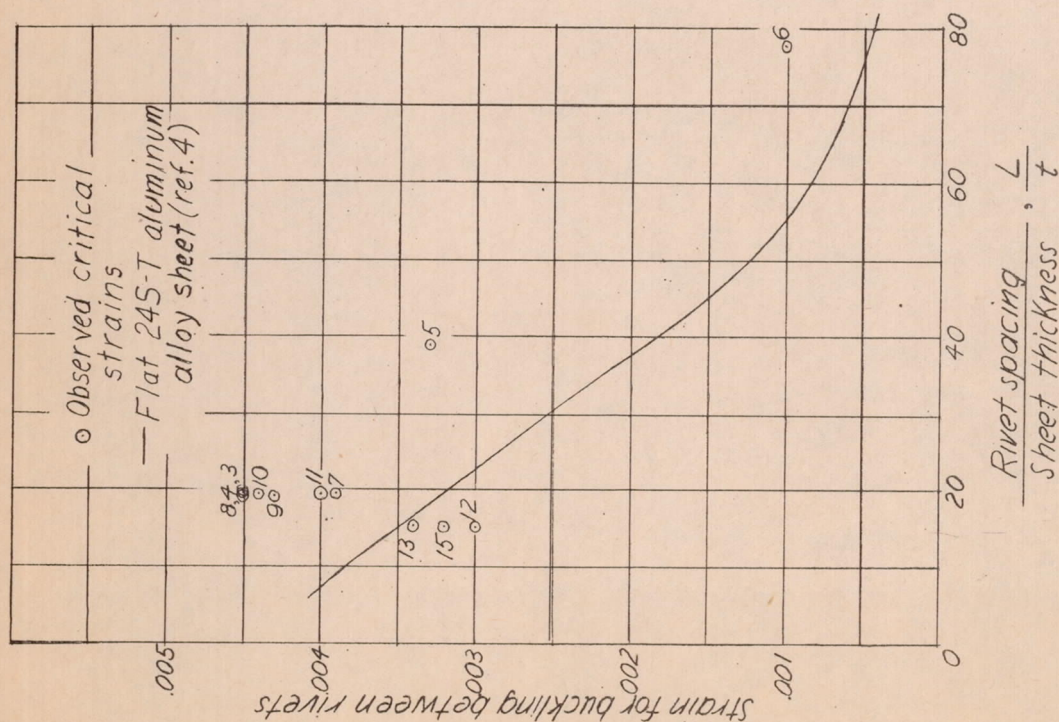
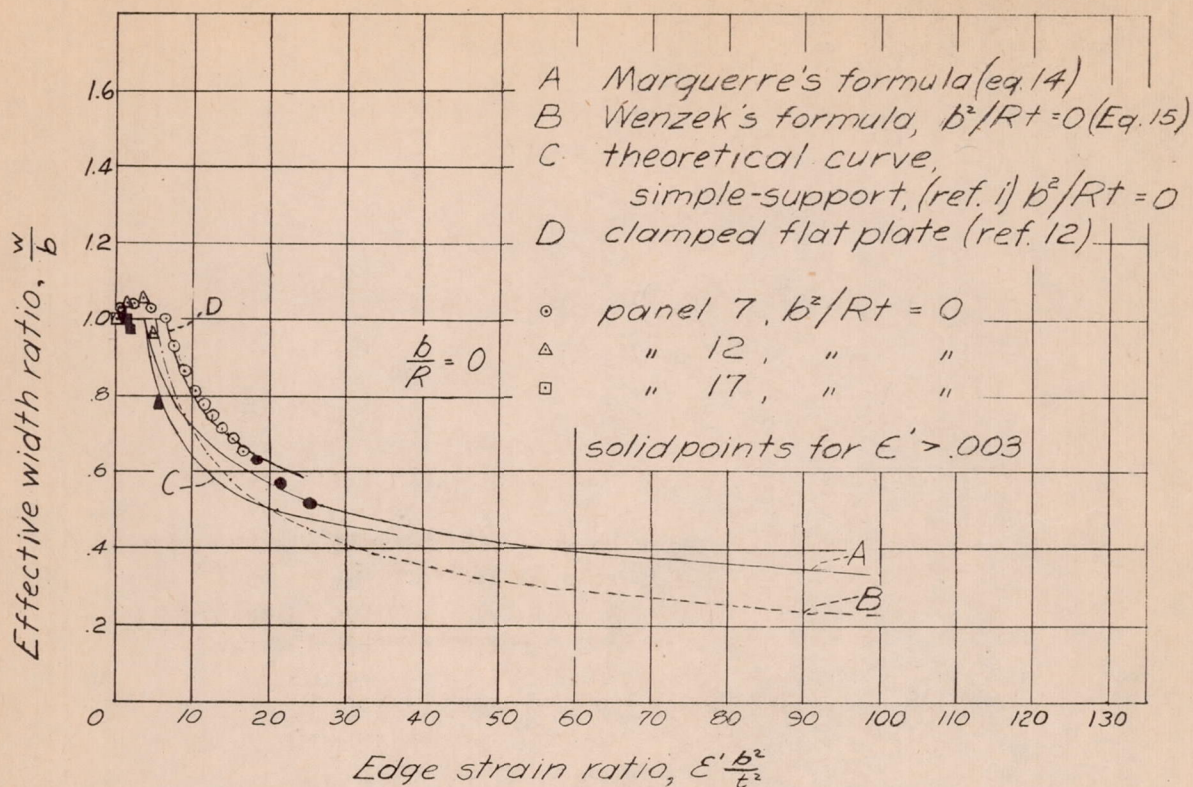Lundquist and Schuette

Figure 31.- Buckling between rivets.

Figure 32.- Effective width ratio of observed data, Marguerre's
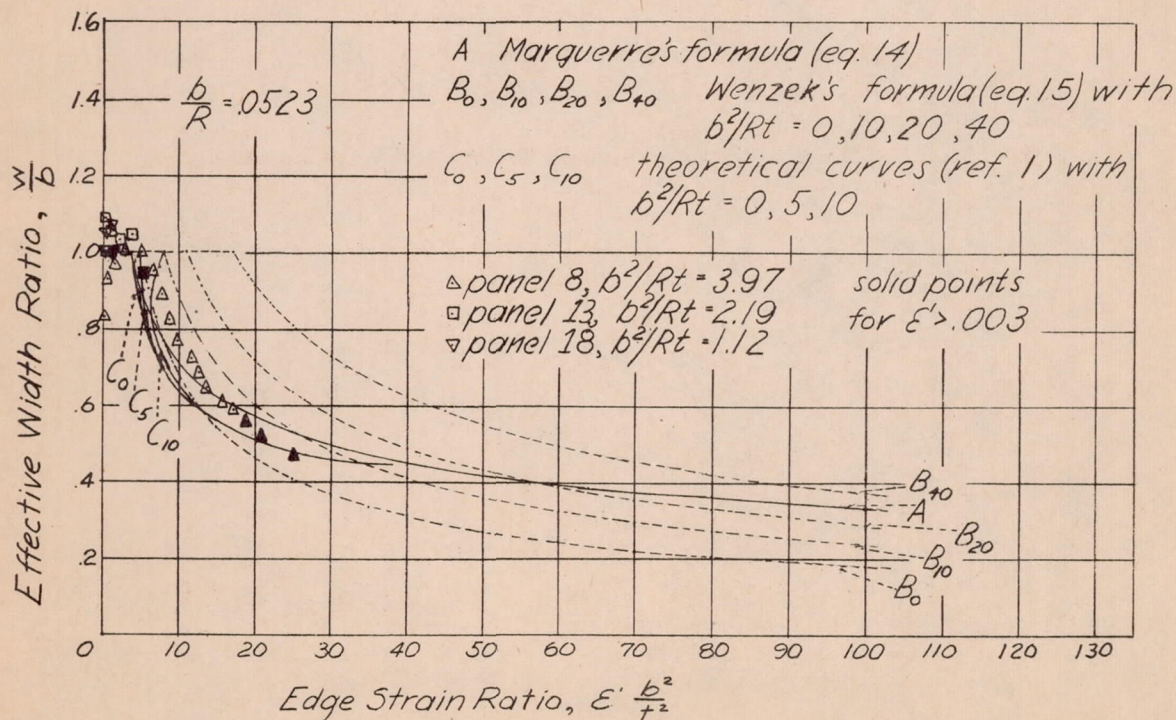formula, Wenzek's formula, and theoretical curves
(references 1 and 12), b/R = 0.

Figure 33.- Effective width ratio of observed data, Marguerre's
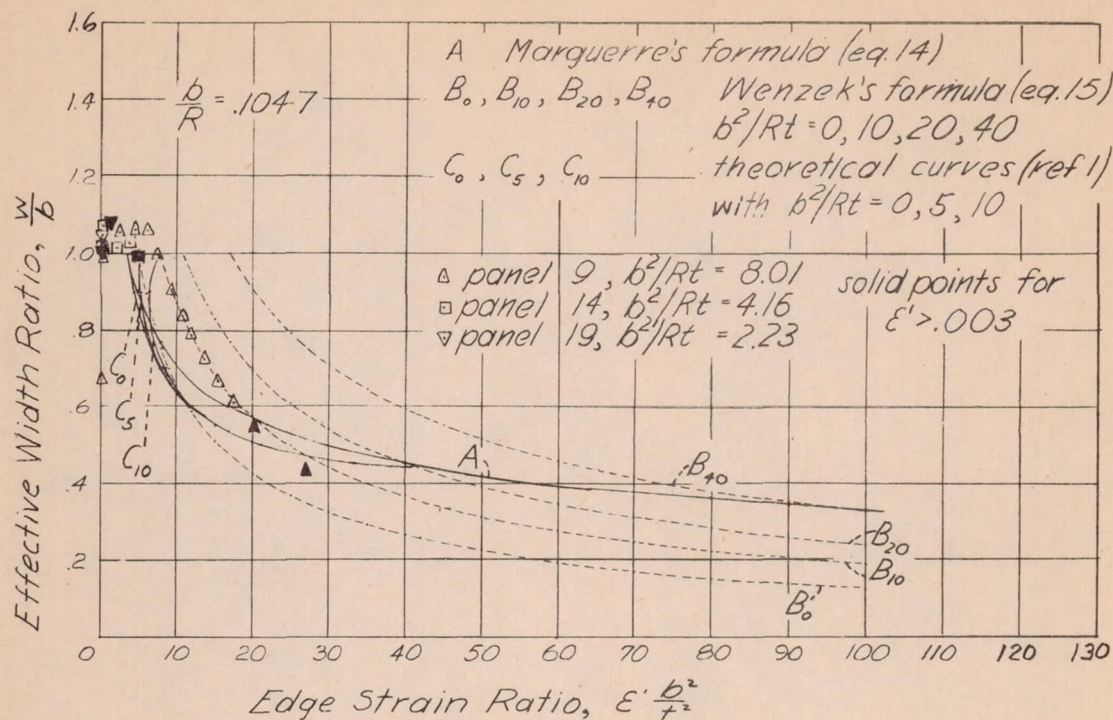formula, Wenzek's formula, and theoretical curves
(reference 1), b/R = 0.0523.

Figure 34.- Effective width ratio of observed data, Marguerre's
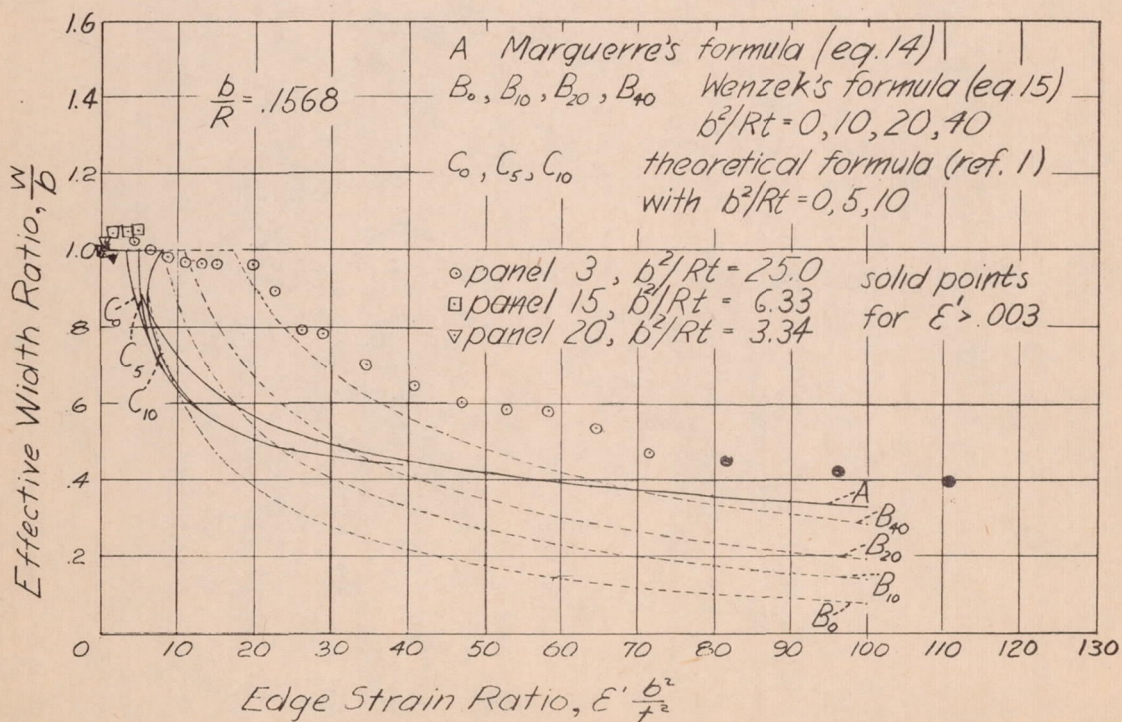formula, Wenzek's formula, and theoretical curves
(reference 1), b/R = 0.1047.

Figure 35.- Effective width ratio of observed data, Marguerre's
formula, Wenzek's formula, and theoretical curves
(reference 1), b/R = 0.1568.

A   Marguerre's formula (eq.14)

B_0, B_{10}, B_{20}, B_{40} Wenzek's formula (eq. 15)
        b^2/Rt = 0, 10, 20, 40

C_0, C_5, C_{10} theoretical curves (ref. 1)
        with b^2/Rt = 0, 5, 10

$\dfrac{b}{R}$ = .2092

○ panel 4 , b^2/Rt = 32.6
△ panel 5 , b^2/Rt = 32.6
▽ panel 6 , b^2/Rt = 32.6
▢ panel 11 , b^2/Rt = 16.0
▷ panel 16 , b^2/Rt = 8.26
◁ panel 21 , b^2/Rt = 4.41

solid points for $\varepsilon' > .003$

Effective Width Ratio, $\dfrac{w}{b}$
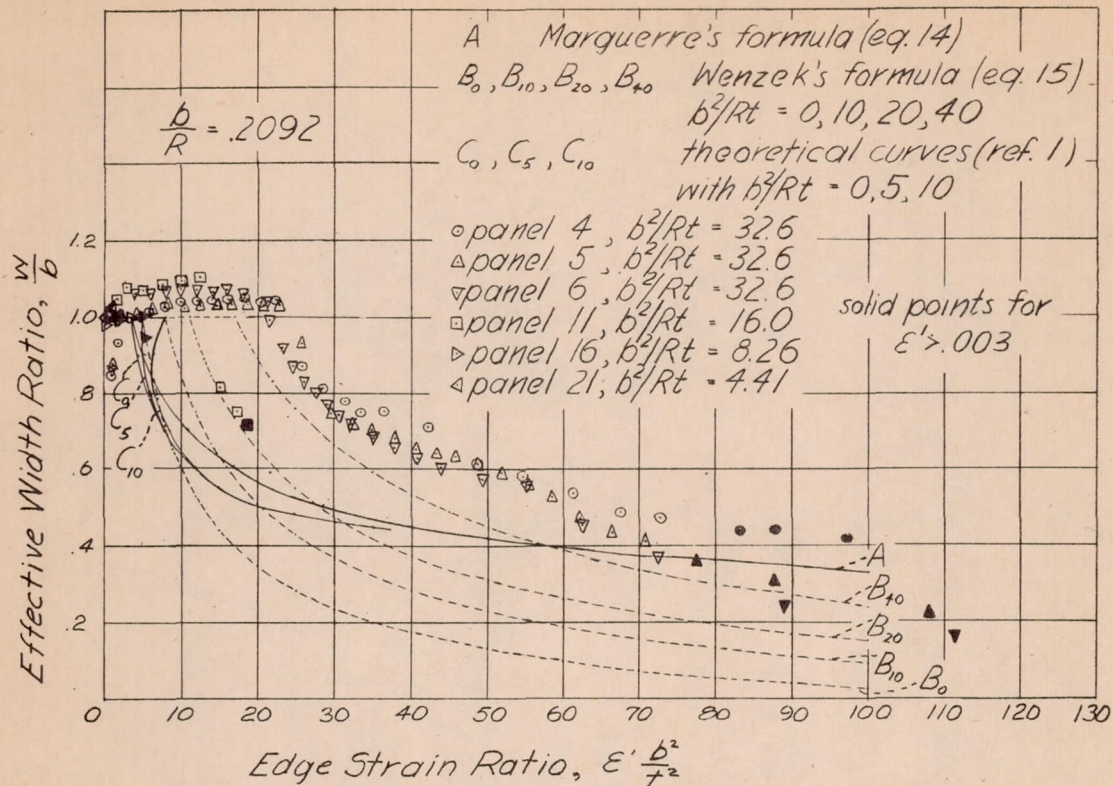
Edge Strain Ratio, $\varepsilon' \dfrac{b^2}{t^2}$

Figure 36.- Effective width ratio of observed data, Marguerre's
        formula, Wenzek's formula, and theoretical curves
(reference 1), b/R = 0.2092.

Observed maximum loads, lbs.

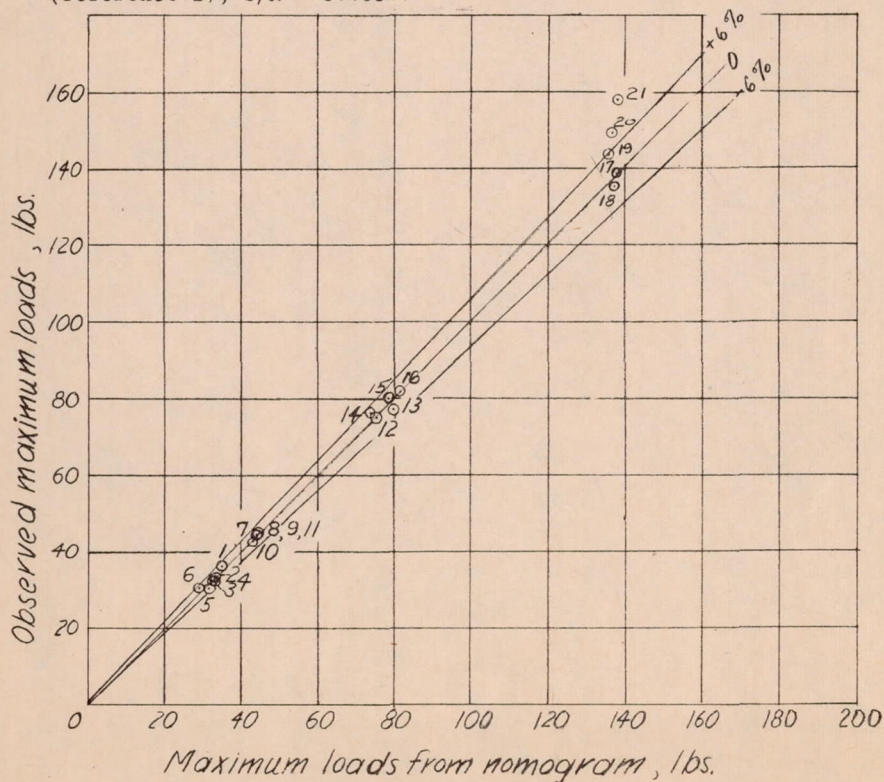Maximum loads from nomogram, lbs.

Figure 37.- Measured maximum loads against loads given by
        nomogram (figure 56 of reference 4).